

# **Integrated HydroKinetic Model: First steps from the LHC towards NICA energies**

---

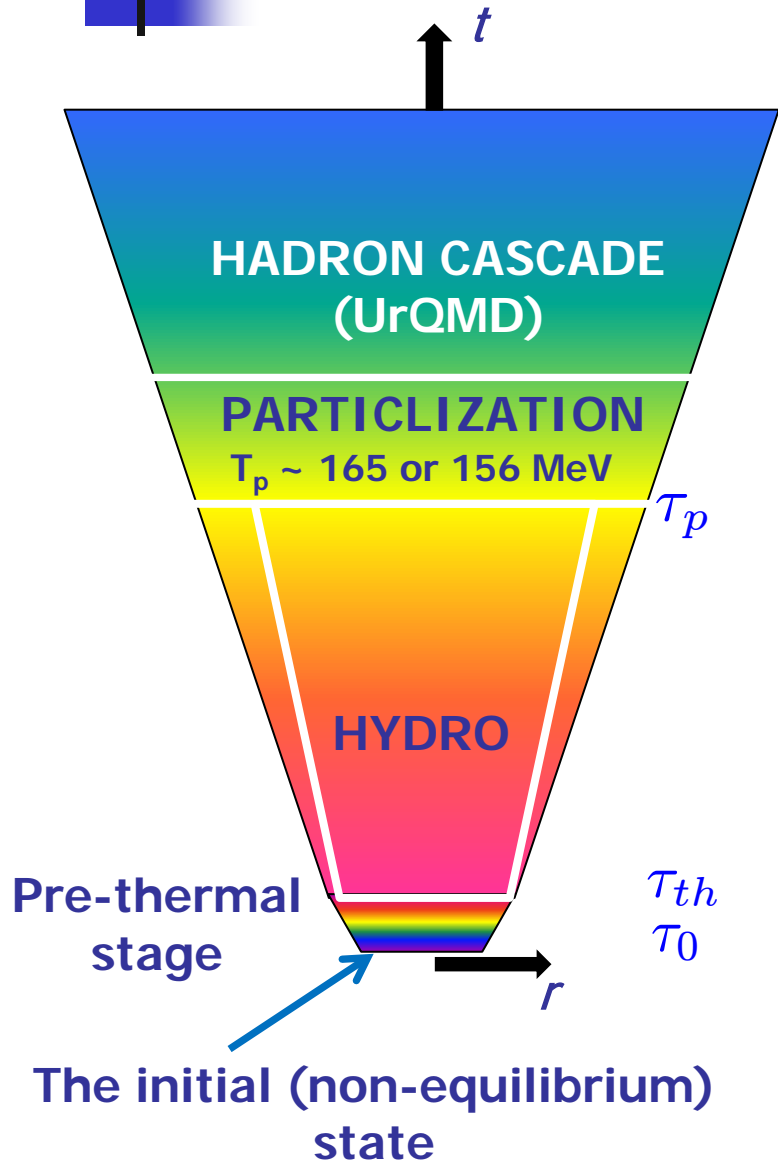
**Yuri Sinyukov**

**Bogolyubov Institute, Kiev**

**April 16-18 2018, JINR Dubna**

**II International Workshop on simulations for NICA energies**

# Integrated HydroKinetic model: HKM → iHKM



Complete algorithm incorporates the stages:

- generation of the initial states;
- thermalization of initially non-thermal matter;
- **viscous** chemically equilibrated hydrodynamic expansion;
- **sudden** (with option: continuous) particlization of expanding medium;
- a switch to UrQMD cascade with near equilibrium hadron gas as input;
- simulation of observables.

Yu.S., Akkelin, Hama: PRL 89 (2002) 052301;

... + Karpenko: PRC 78 (2008) 034906;

Karpenko, Yu.S. : PRC 81 (2010) 054903;

... PLB 688 (2010) 50;

Akkelin, Yu.S. : PRC 81 (2010) 064901;

Karpenko, Yu.S., Werner: PRC 87 (2013) 024914;

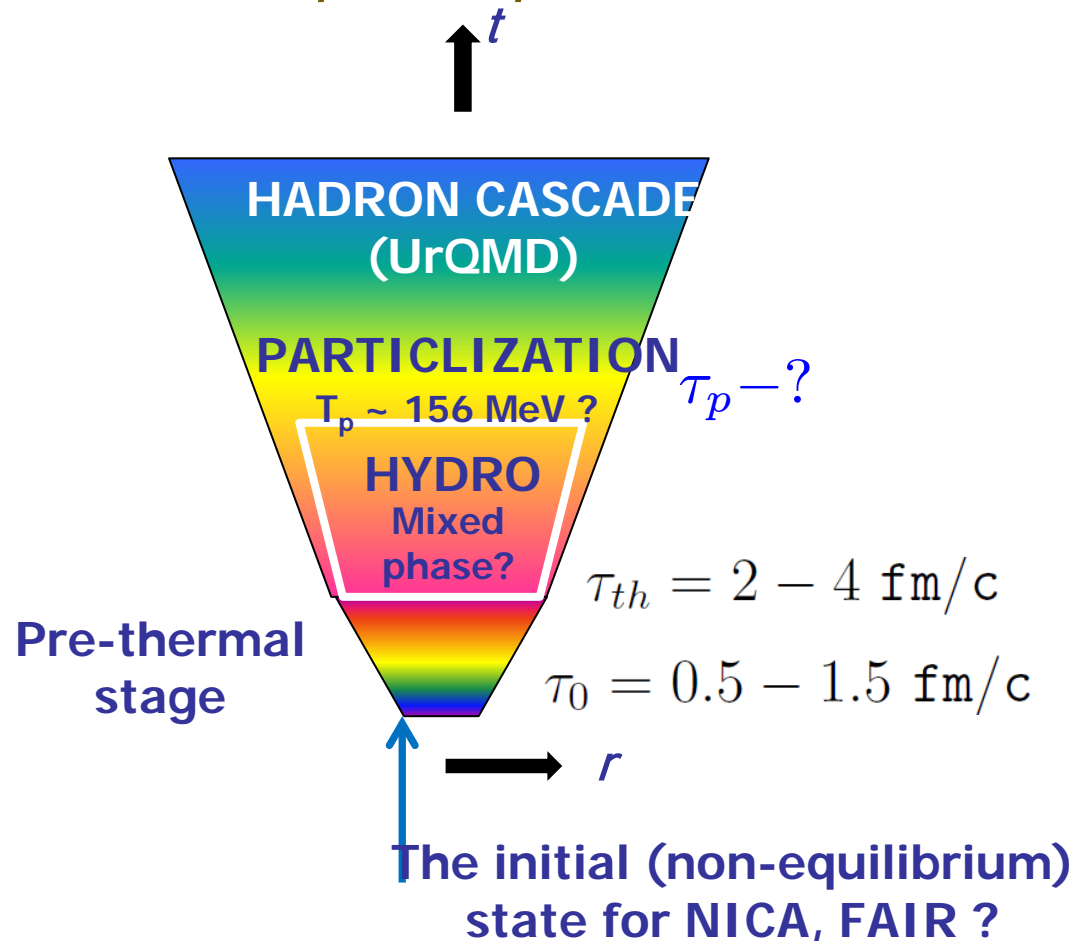
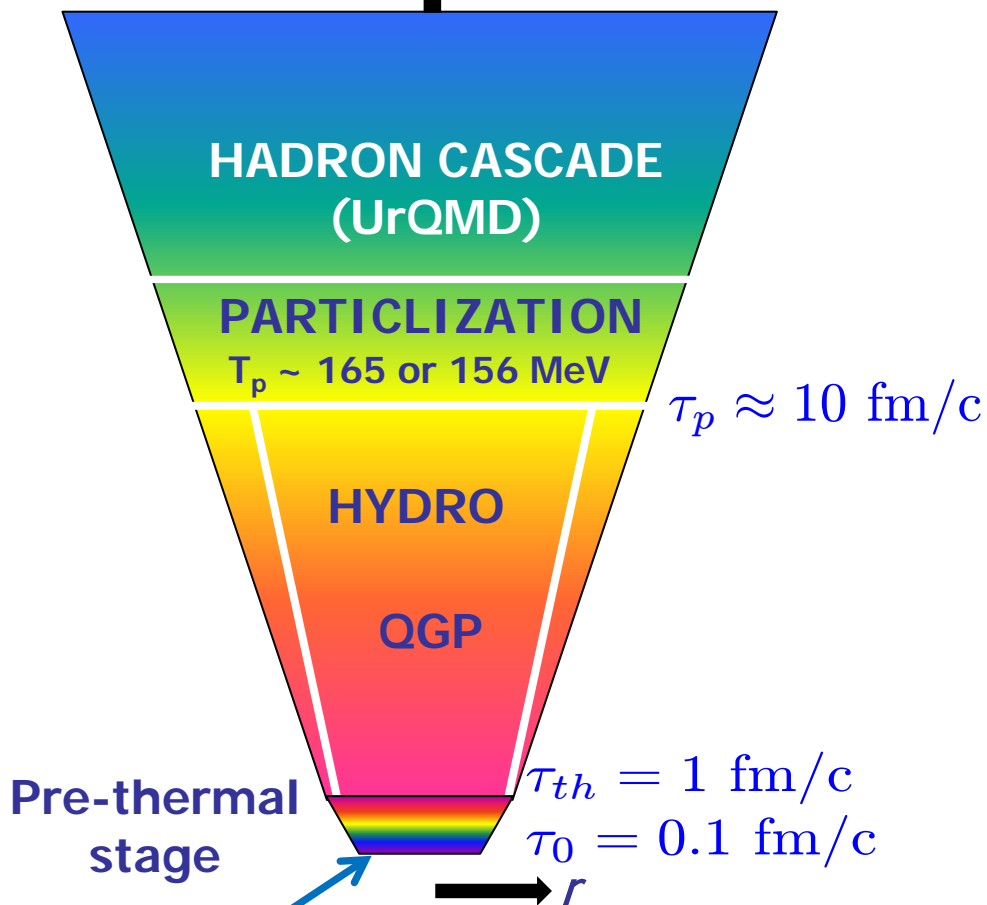
Naboka, Akkelin, Karpenko, Yu.S. : PRC **91** (2015) 014906;

Naboka, Karpenko, Yu.S. Phys. Rev. C **93** (2016) 024902.

# Space-time carton of A+A collisions:

LHC, top RHIC

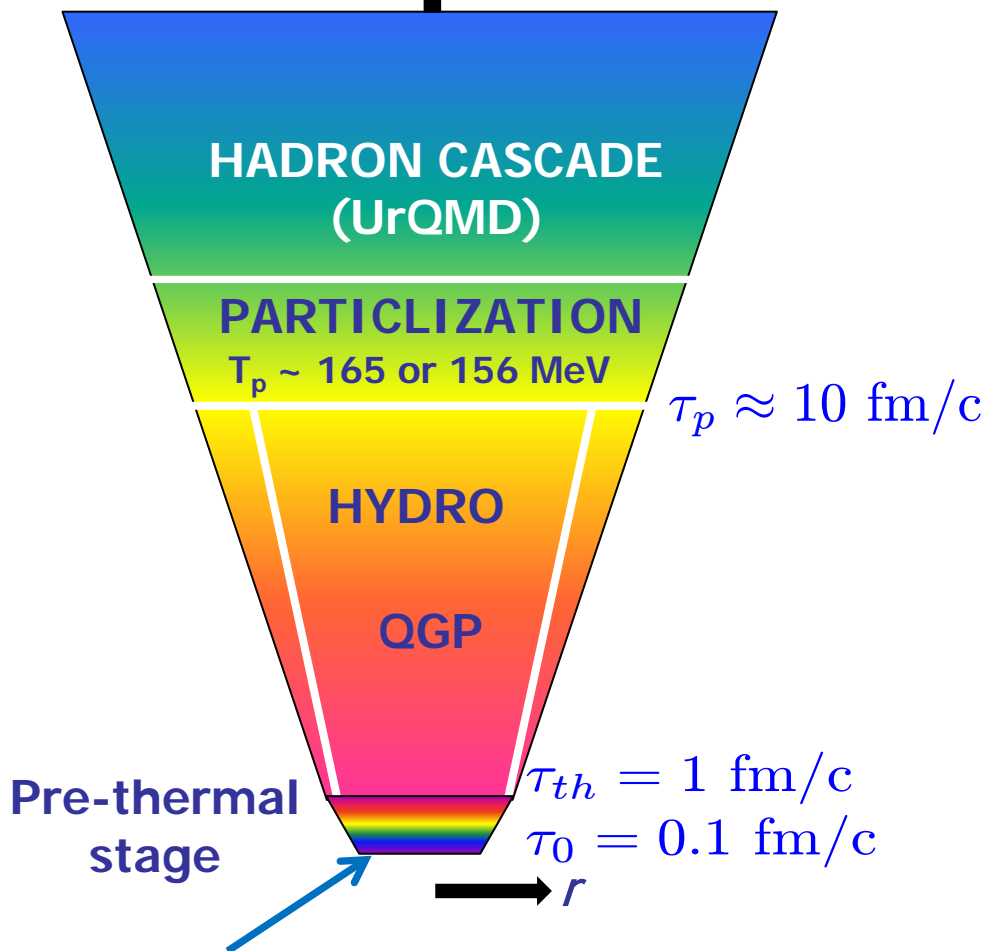
NICA, FAIR, RHIC BES



# Space-time carton of A+A collisions:

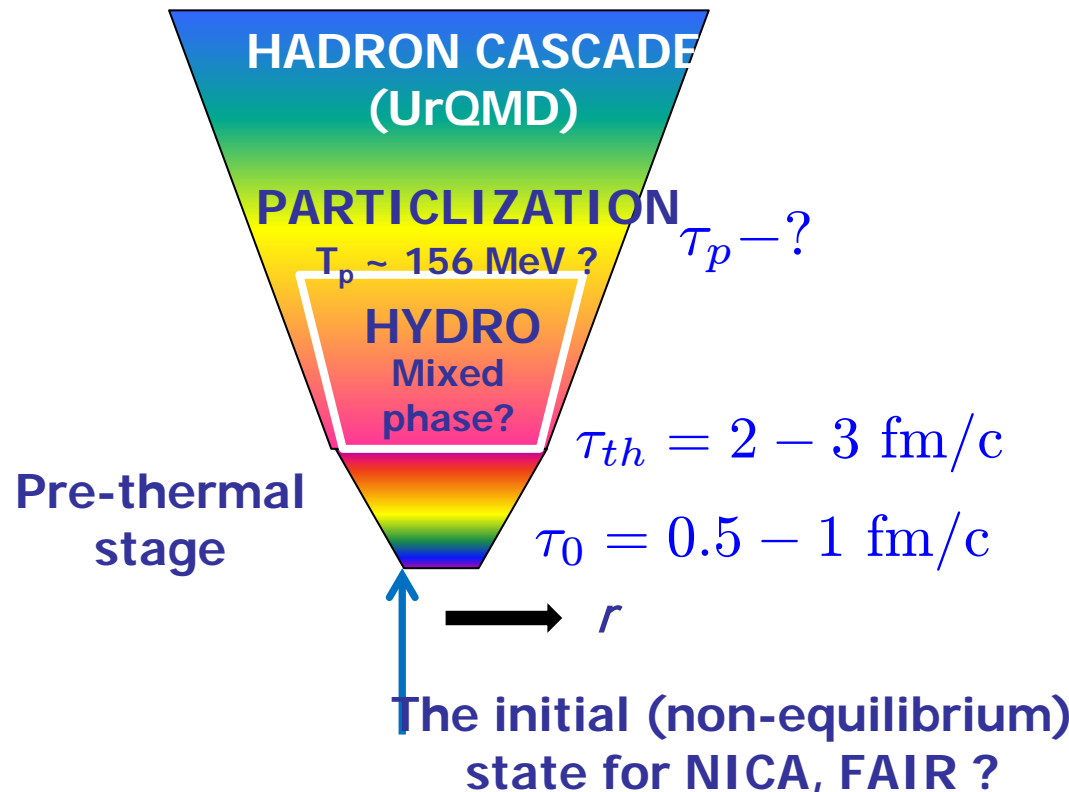
LHC, top RHIC

NICA, FAIR, RHIC BES



The initial (non-equilibrium) state for top RHIC, LHC

Small (zero) baryon chemical potentials



EoS

Large baryon chemical potentials



# Initial states

The most commonly used models of initial state are:

## High Energies

MC-G (Monte Carlo Glauber)  
MC-KLN (Monte Carlo Kharzeev-Levin-Nardi)  
EPOS (parton-based Gribov-Regge model)  
EKRT (perturbative QCD + saturation model)  
IP-Glasma (Impact Parameter dependent Glasma)

## Low Energies

MC-G (Monte Carlo Glauber) - ?  
UrQMD (Ultra-Relativistic Molecular Dynamics) - ?  
.... ?

## PROBLEM:

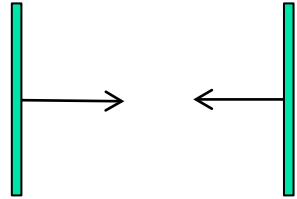
**No one model leads to the proper matter thermalization,  
while**

**the biggest experimental discovery for a few decades is that hydrodynamics is the basis  
of the "Standard Model " of high energy A+A collisions**

High

and

Low energies



$$\gamma\text{-factor} = \frac{\sqrt{s_{NN}}}{2m_p}$$

$$y_{beam} = \text{arcosh}(\gamma)$$

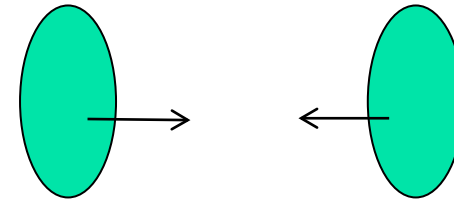
$$v_{beam} = \tanh(y_{beam})$$

LHC,  $\sqrt{s_{NN}} = 5.02$  TeV,

$\gamma\text{-factor} = 2500$

$y_{beam} = 8.5$

Overlapping time  $3 \times 10^{-3}$  fm/c



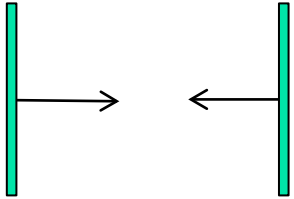
NICA,  $\sqrt{s_{NN}} = 9$  GeV,

$\gamma\text{-factor} = 4.5$

$y_{beam} = 2.2$

Overlapping time 1.6 fm/c

# High and Low energies



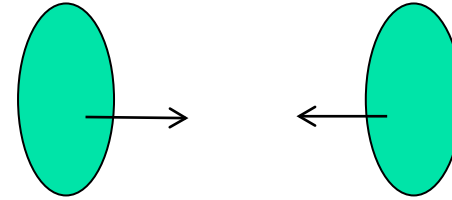
LHC,  $\sqrt{s_{NN}} = 5.02$  TeV,

$$\gamma\text{-factor} = \frac{\sqrt{s_{NN}}}{2m_p}$$

$$y_{beam} = \text{arcosh}(\gamma)$$

$$v_{beam} = \tanh(y_{beam})$$

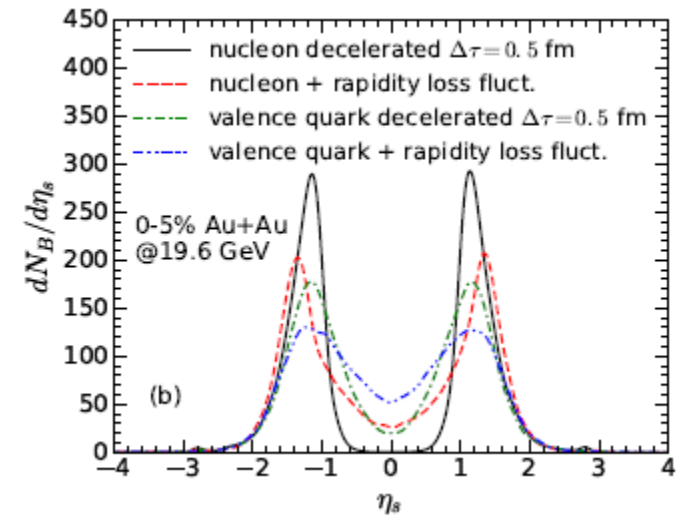
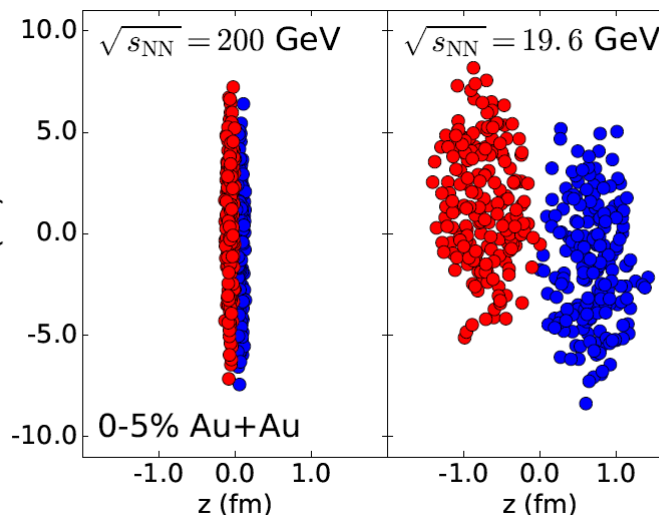
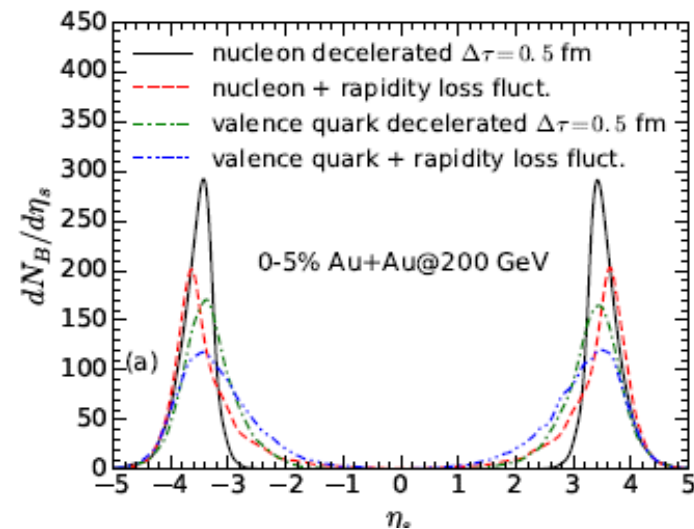
**RHIC BES**



NICA,  $\sqrt{s_{NN}} = 9$  GeV,

$$\eta_s = \frac{1}{2} \ln \frac{t+z}{t-z}, \quad \tau = \sqrt{t^2 - z^2} \quad \longrightarrow \quad t = \tau \cosh \eta_s, \quad z = \tau \sinh \eta_s$$

Chun Shen and Björn Schenke 2017, 2018



# Chemical potential at particlization hypersurface $T=165$ MeV

For initially two-humped baryon density structure

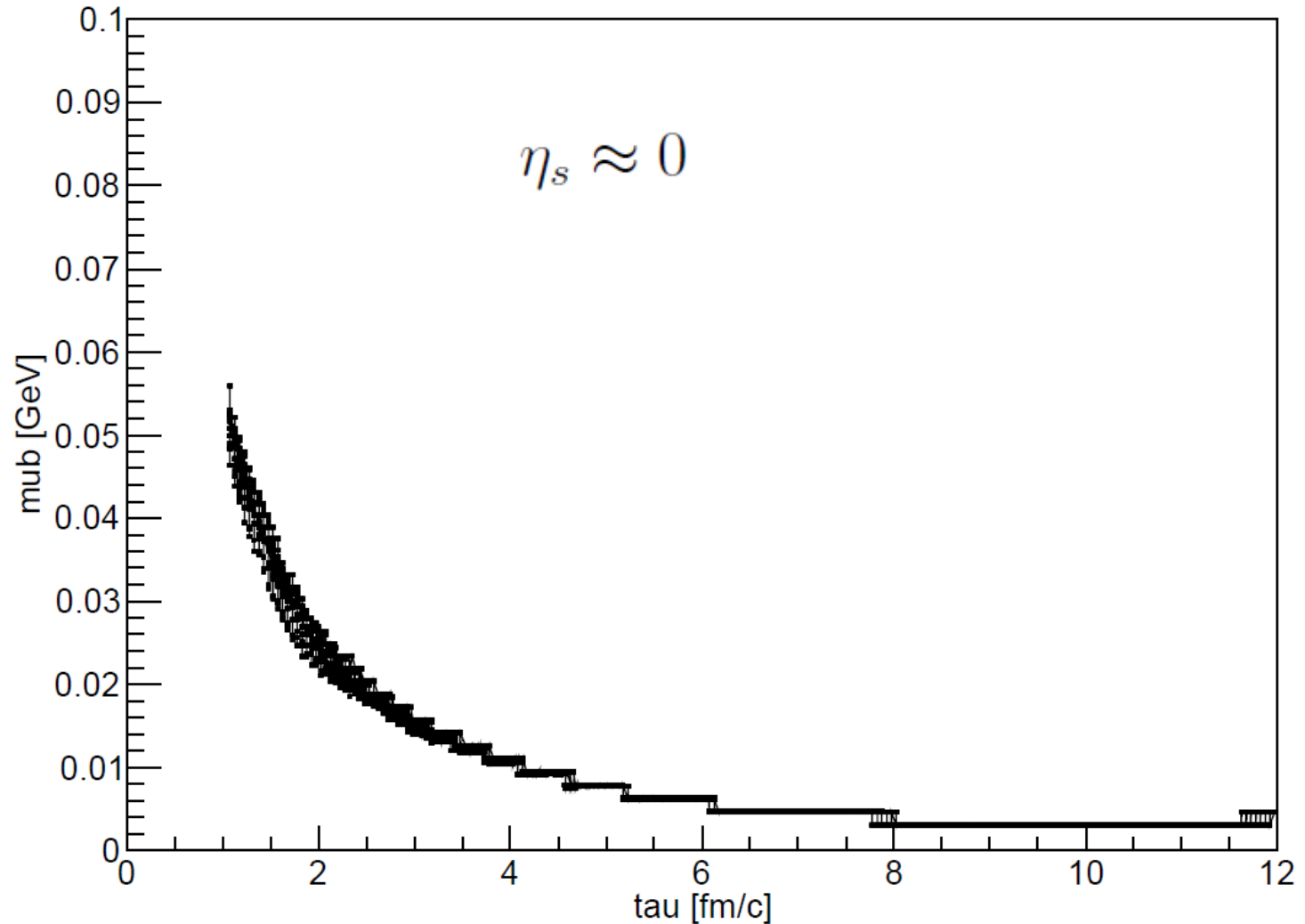


Рис. 1:  $\mu_b(\tau)$  dependence on the hypersurface of constant temperature  $T = 165$  MeV.  $\sigma_t = 6.5$  fm,  $\sigma_l = 1.0$  fm,  $\eta_c = 1.5$ . Only hypersurface elements with  $\eta \approx 0$  are considered. Initial total baryon charge  $N_b \approx 400$



# Chemical potential at particlization hypersurface

$$\left. \begin{array}{l} T=165 \text{ MeV} \\ r_T(\tau) \end{array} \right\}$$

For initially two-humped baryon density structure

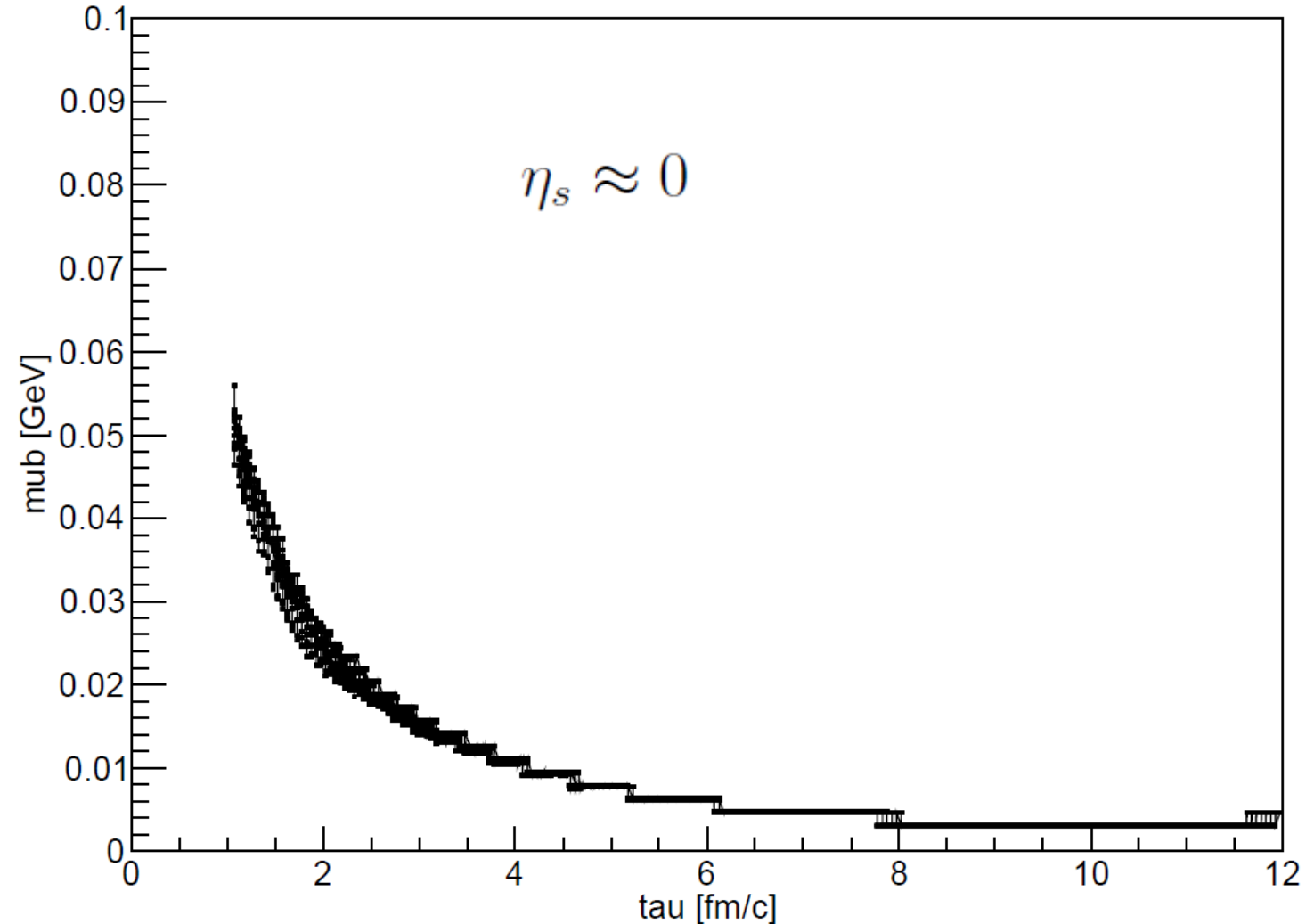


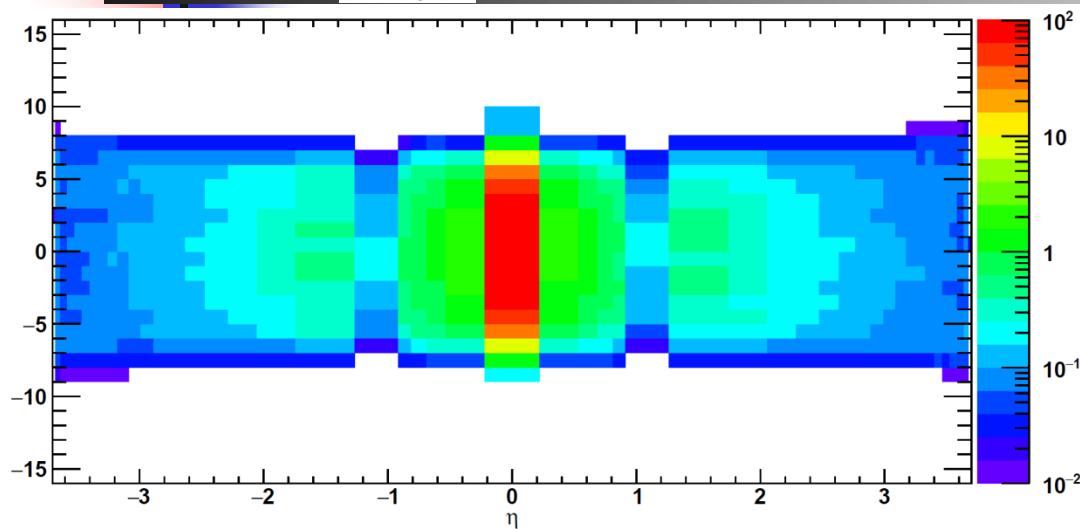
Рис. 1:  $\mu_b(\tau)$  dependence on the hypersurface of constant temperature  $T = 165 \text{ MeV}$ .  $\sigma_t = 6.5 \text{ fm}$ ,  $\sigma_l = 1.0 \text{ fm}$ ,  $\eta_c = 1.5$ . On hypersurface elements with  $\eta \approx 0$  are considered. Initial total baryon charge  $N_b \approx 400$

**Simple conclusion:**

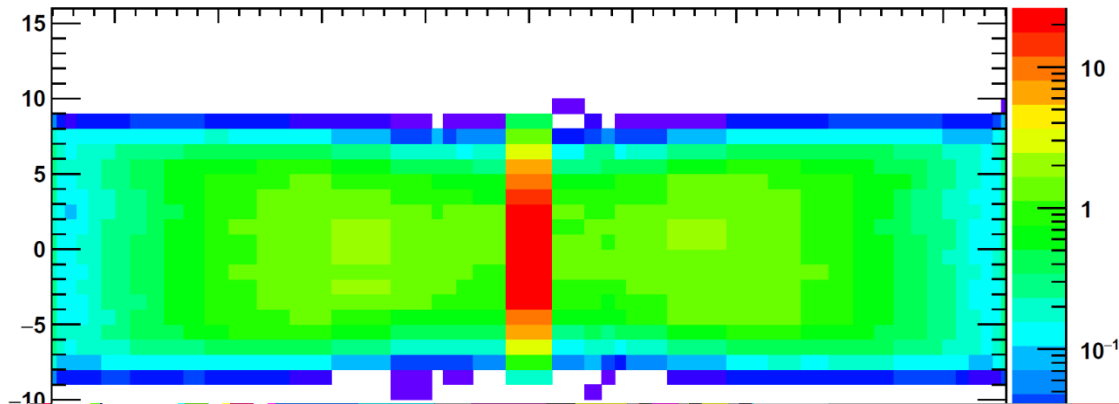
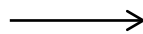
the so-called thermal models with  $\mu$ ,  $T$  to be constant at chemical freeze-out are hardly applicable for baryon rich matter

$$\frac{dN_B}{d\eta_s}$$

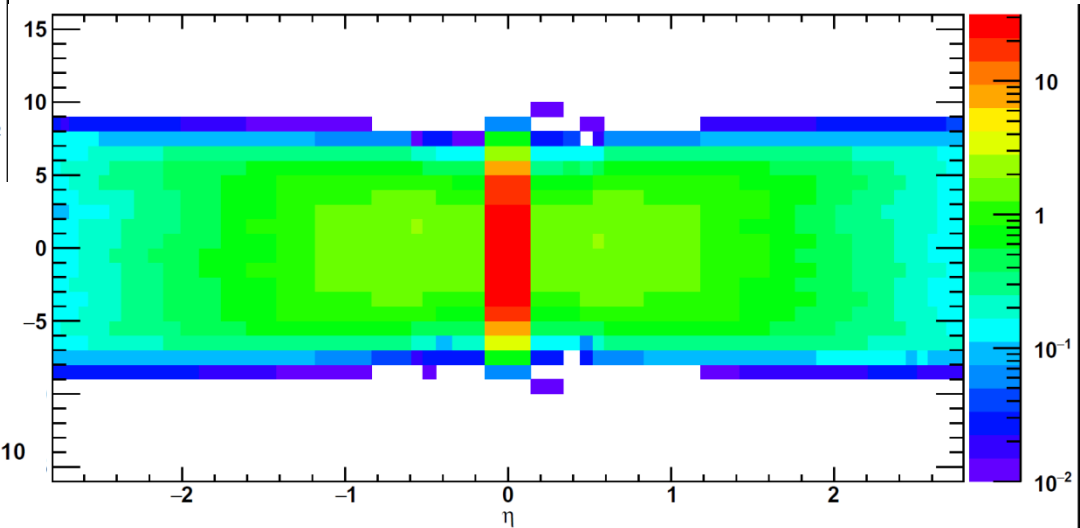
UrQMD, Au+Au,  $\sqrt{s_{NN}} = 27$  GeV



$\tau = 2.5$  fm/c



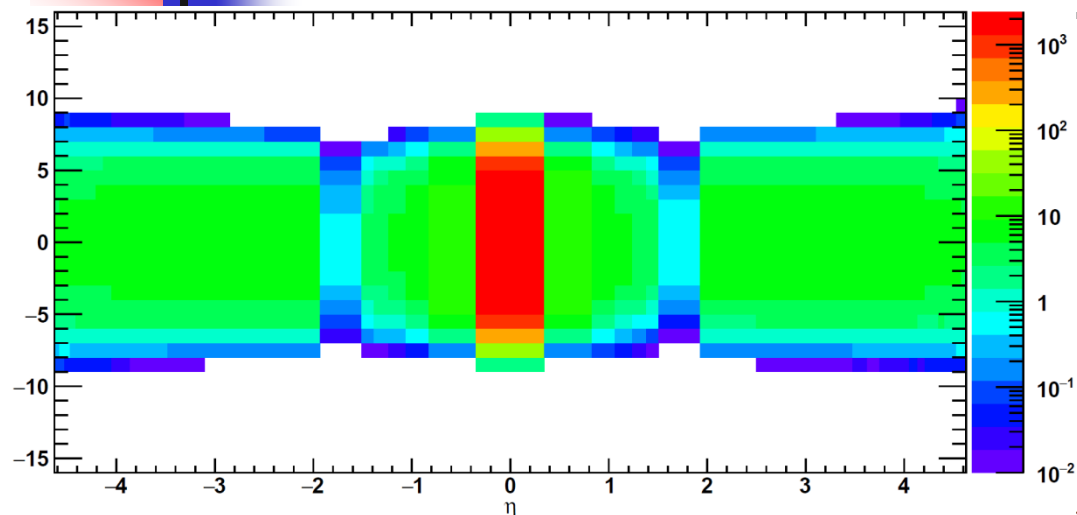
←  $\tau = 1$  fm/c



←  $\tau = 4$  fm/c

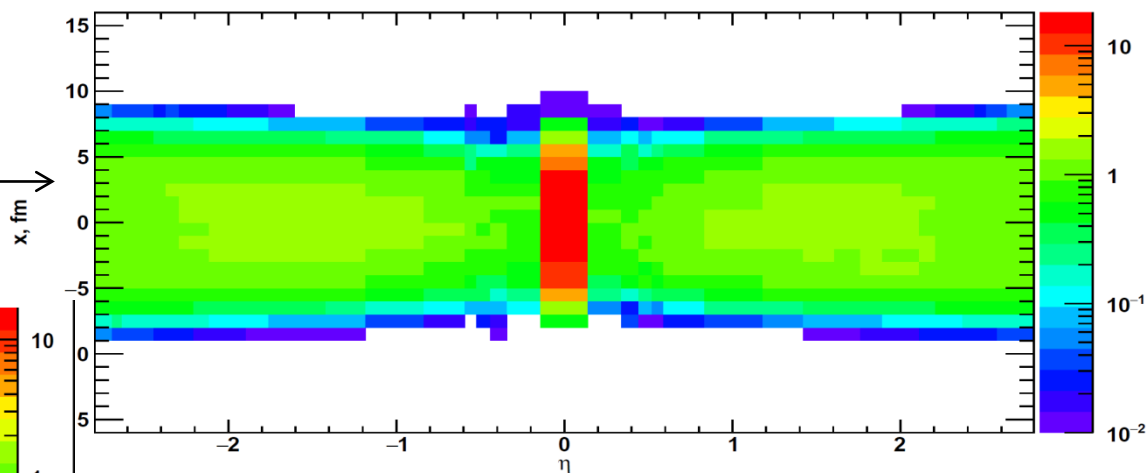
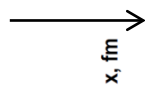
$$\frac{dN_B}{d\eta_s}$$

UrQMD, Au+Au,  $\sqrt{s_{NN}} = 62$  GeV

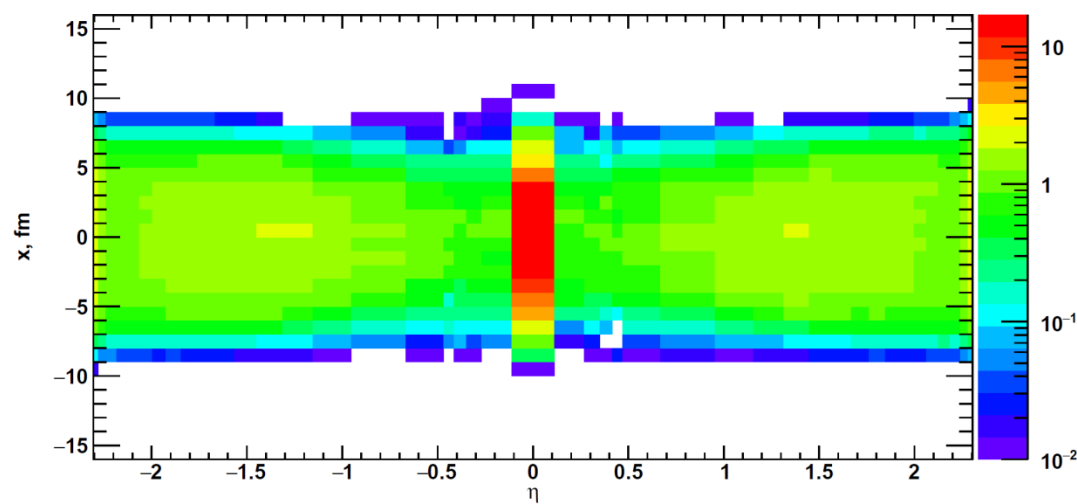


←  $\tau = 0.4$  fm/c

$\tau = 2.5$  fm/c

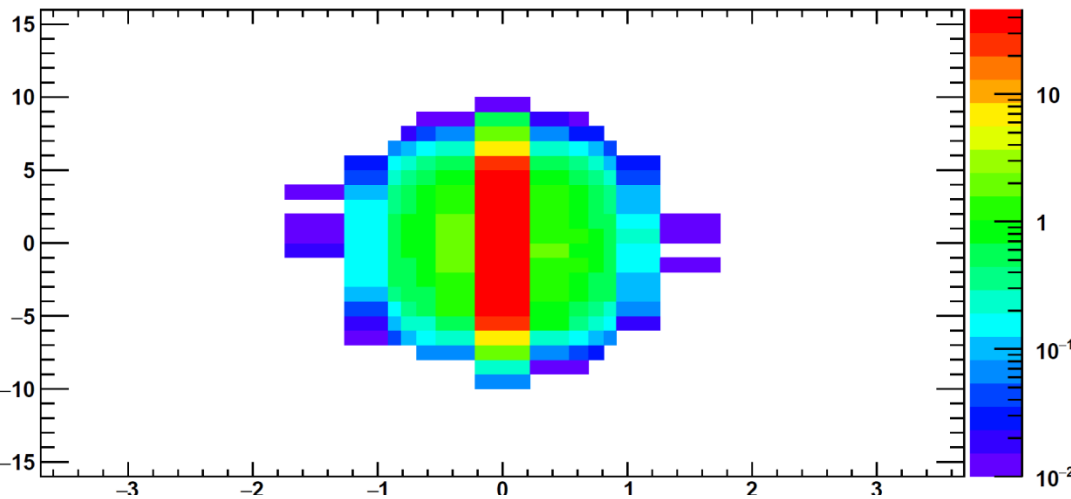


←  $\tau = 4$  fm/c



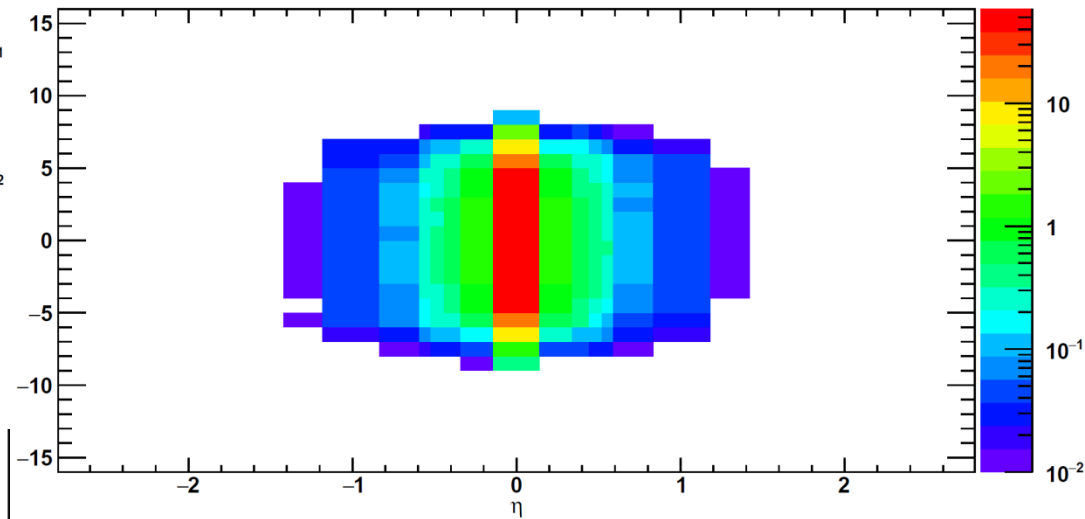
$$\frac{dN_B}{d\eta_s}$$

UrQMD, Au+Au,  $\sqrt{s_{NN}} = 9$  GeV

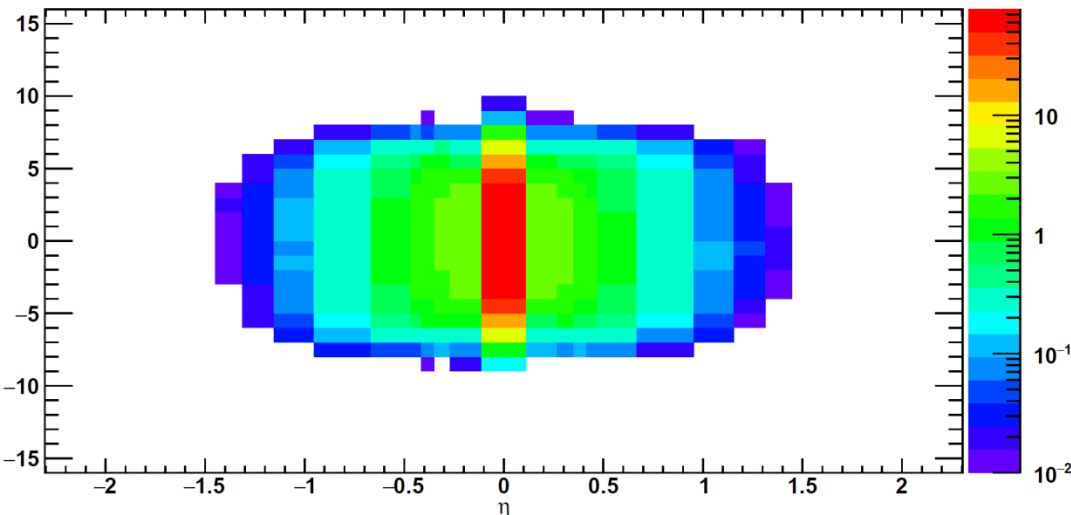


←  $\tau = 1$  fm/c

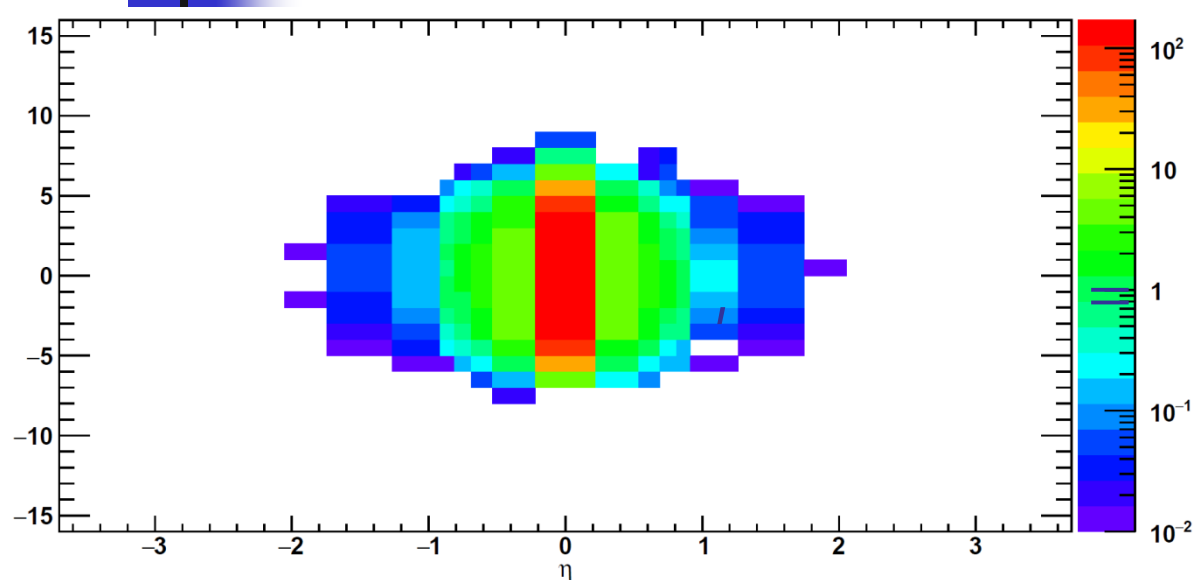
$\tau = 2.5$  fm/c →



←  $\tau = 4$  fm/c



# When does thermalization process start?

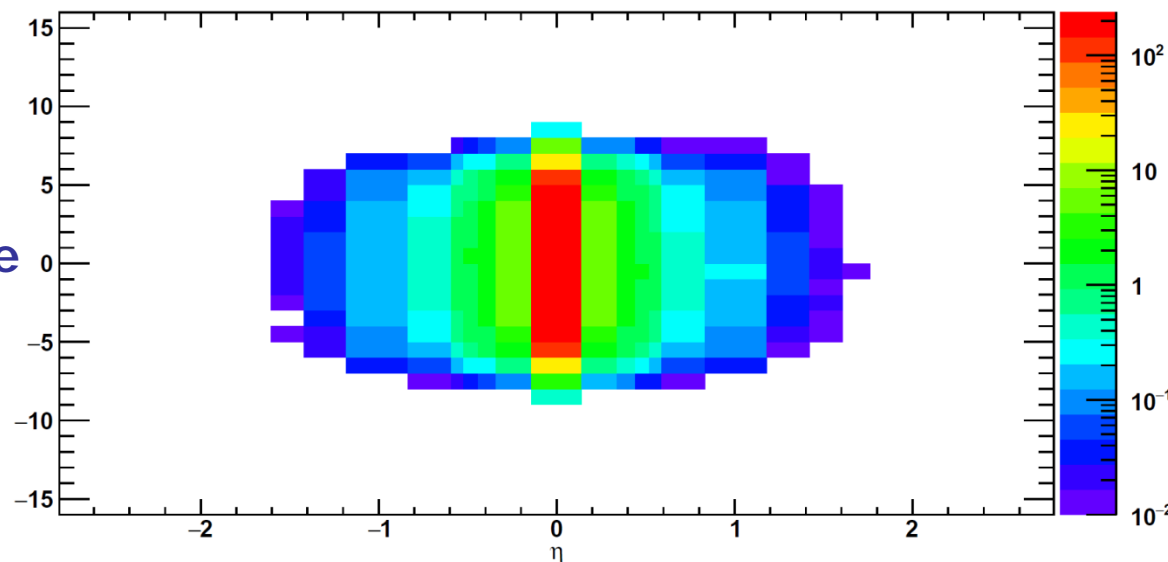


Energy density vs space-time rapidity,

$$\sqrt{s_{NN}} = 9 \text{ GeV}$$

←  $\tau = 1 \text{ fm/c}$

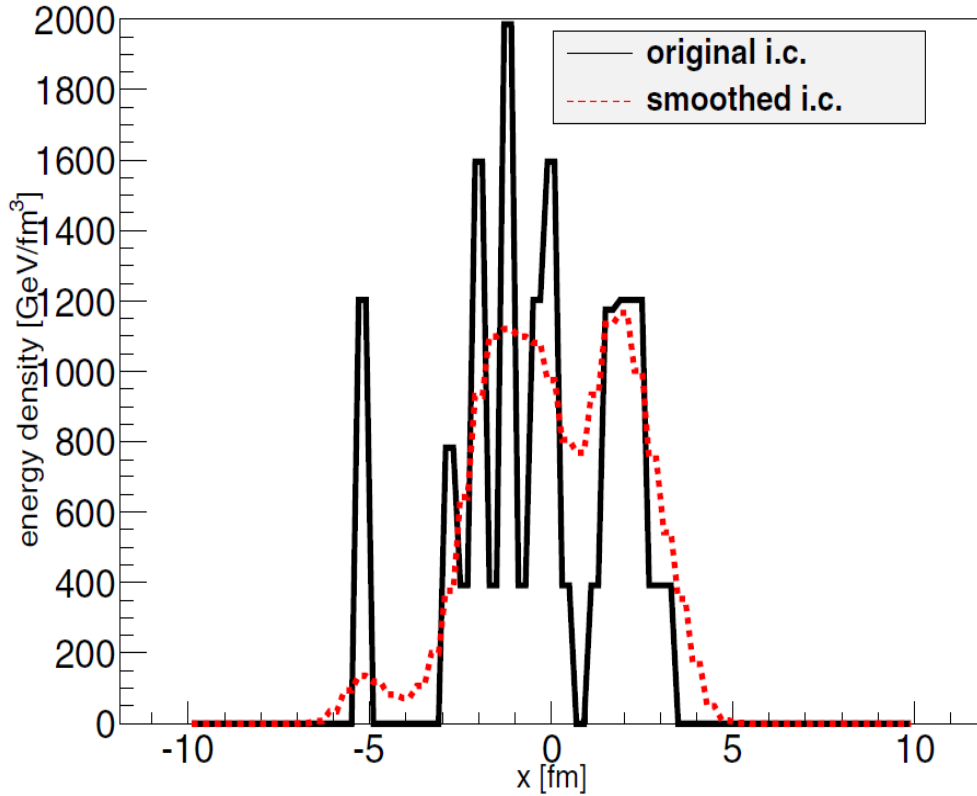
$\tau = 2.5 \text{ fm/c}$  →



The initial energy density formation time  $\tau_0$  at NICA energy is agreed with overlapping time 1.5- 2.0 fm/c

# MC-G Initial State (IS) attributed to $\tau_0 = 0.1 \text{ fm}/c$

## GLISSANDO 2



- The initial state (IS) is highly inhomogeneous.
- It is not locally equilibrated.
- The IS most probable is strongly momentum anisotropic (result from CGC)

$$f(t_{\sigma_0}, \mathbf{r}_{\sigma_0}, \mathbf{p}) = \epsilon(b; \tau_0, \mathbf{r}_T) f_0(p)$$

$$T_0^{\mu\nu}(x) = \int d^3p \frac{p^\mu p^\nu}{p_0} f_{\sigma_0}(x, p); T^{00}[f_0(p)] = 1$$

$$f_0^*(p) \propto \exp\left(-\sqrt{\frac{p_T^2}{\lambda_\perp^2} + \frac{p_L^2}{\lambda_\parallel^2}}\right) \quad \text{Florkowski et al}$$

### MC-G Hybrid for ensemble of ISs :

$$\epsilon(b; \tau_0, \mathbf{r}_T) = \epsilon_0 \frac{(1 - \alpha) N_W(b, \mathbf{r}_T)/2 + \alpha N_{bin}(b, \mathbf{r}_T)}{(1 - \alpha) N_W(b = 0, \mathbf{r}_T = 0)/2 + \alpha N_{bin}(b = 0, \mathbf{r}_T = 0)}$$

### Parameters of IS

$$\Lambda = \lambda_\perp / \lambda_\parallel$$

$$\epsilon_0, \alpha = 0.24 \quad 14$$

# Pre-thermal stage (thermalization)

Akkelin, Yu.S. :PRC **81** (2010); Naboka, Akkelin, Karpenko, Yu.S. : PRC **91** (2015).

Non-thermal state at  $\tau_0$   $\longrightarrow$  locally near equilibrated state at  $\tau_{th}$

Boltzmann equation in  
relaxation time approximation  
(integral form)

**MAIN OBJECT**

$$\mathcal{P}_\sigma(x, p) = \exp\left(-\int_t^{t_\sigma} \frac{d\bar{t}}{\tau_{rel}(\bar{x}, p)}\right)$$
$$\bar{x} \equiv (\bar{t}, \mathbf{x}_\sigma + (\mathbf{p}/p_0)(\bar{t} - t_\sigma))$$

# Pre-thermal stage (thermalization)

Akkelin, Yu.S. :PRC **81** (2010); Naboka, Akkelin, Karpenko, Yu.S. : PRC **91** (2015).

Non-thermal state  $\tau_0 = 0.1 \text{ fm}/c \longrightarrow$  locally near equilibrated state  $\tau_{th} = 1 \text{ fm}/c$

Boltzmann equation in  
relaxation time approximation  
(integral form)

**MAIN OBJECT**

$$\mathcal{P}_\sigma(x, p) = \exp\left(-\int_{t_\sigma}^{\bar{t}} \frac{d\bar{t}}{\tau_{rel}(\bar{x}, p)}\right)$$

$$\bar{x} \equiv (\bar{t}, \mathbf{x}_\sigma + (\mathbf{p}/p_0)(\bar{t} - t_\sigma))$$

**MAIN ANSATZ with minimal number of parameters:**  $\tau_0, \tau_{th}, \tau_{rel}$

$$\mathcal{P}_{\tau_0 \rightarrow \tau}(\tau) = \left( \frac{\tau_{th} - \tau}{t_{th} - \tau_0} \right)^{\frac{\tau_{th} - \tau_0}{\tau_{rel}(\tau_0)}} \longrightarrow T^{\mu\nu}(x) = T_{\text{free}}^{\mu\nu}(x)\mathcal{P}(\tau) + T_{\text{hyd}}^{\mu\nu}(x)(1 - \mathcal{P}(\tau))$$

$$\longrightarrow 0 \leq \mathcal{P}(\tau) \leq 1, \mathcal{P}(\tau_0) = 1, \mathcal{P}(\tau_{th}) = 0, \partial_\mu \mathcal{P}(\tau)_{\tau_{th}} = 0$$



# Pre-thermal stage (thermalization)

Akkelin, Yu.S. :PRC **81** (2010); Naboka, Akkelin, Karpenko, Yu.S. : PRC **91** (2015).

Non-thermal state  $\tau_0 = 0.1 \text{ fm}/c \longrightarrow$  locally near equilibrated state  $\tau_{th} = 1 \text{ fm}/c$

Boltzmann equation in  
relaxation time approximation  
(integral form)

**MAIN OBJECT**

$$\mathcal{P}_\sigma(x, p) = \exp\left(-\int_{t_\sigma}^{\bar{t}} \frac{d\bar{t}}{\tau_{rel}(\bar{x}, p)}\right)$$

$$\bar{x} \equiv (\bar{t}, \mathbf{x}_\sigma + (\mathbf{p}/p_0)(\bar{t} - t_\sigma))$$

**MAIN ANSATZ with minimal number of parameters:**  $\tau_0, \tau_{th}, \tau_{rel}$

$$\mathcal{P}_{\tau_0 \rightarrow \tau}(\tau) = \left( \frac{\tau_{th} - \tau}{t_{th} - \tau_0} \right)^{\frac{\tau_{th} - \tau_0}{\tau_{rel}(\tau_0)}} \longrightarrow T^{\mu\nu}(x) = T_{\text{free}}^{\mu\nu}(x)\mathcal{P}(\tau) + T_{\text{hyd}}^{\mu\nu}(x)(1 - \mathcal{P}(\tau))$$

$$\longrightarrow 0 \leq \mathcal{P}(\tau) \leq 1, \mathcal{P}(\tau_0) = 1, \mathcal{P}(\tau_{th}) = 0, \partial_\mu \mathcal{P}(\tau)_{\tau_{th}} = 0$$

## MAIN EQUATIONS of THERMALIZATION & HYDRODYNAMIZATION

$$\partial_{;\mu} \tilde{T}_{\text{hyd}}^{\mu\nu}(x) = -T_{\text{free}}^{\mu\nu}(x) \partial_{;\mu} \mathcal{P}(\tau) \quad \text{where} \quad \begin{cases} \tilde{T}_{\text{hyd}}^{\mu\nu} = [1 - \mathcal{P}(\tau)] T_{\text{hyd}}^{\mu\nu} \\ \tilde{\pi}^{\mu\nu} = \pi^{\mu\nu} (1 - \mathcal{P}) \end{cases}$$

$$(1 - \mathcal{P}(\tau)) \left\langle u^\gamma \partial_{;\gamma} \frac{\tilde{\pi}^{\mu\nu}}{(1 - \mathcal{P}(\tau))} \right\rangle = -\frac{\tilde{\pi}^{\mu\nu} - (1 - \mathcal{P}(\tau)) \pi_{\text{NS}}^{\mu\nu}}{\tau_\pi} - \frac{4}{3} \tilde{\pi}^{\mu\nu} \partial_{;\gamma} u^\gamma$$

$$\partial_{;\mu} [(1 - \mathcal{P}) J_{B,\text{hyd}}^\mu(x)] = J_{B,\text{free}}^\mu(x) \partial_{;\mu} (1 - \mathcal{P}(\tau))$$

The complicated picture of gradual transition from non-equilibrated form of matter to hydrodynamic one is described in this formalism by only 3 parameters:

- initial formation time for energy density of total number of quanta/particles number that have interacted,  $\mathcal{T}_0$  .
- relaxation time describing the rate thermalization/hydrodynamization  $\mathcal{T}_{rel}$  .
- thermalization time  $\mathcal{T}_{th}$  .

# The other stages: Hydro evolution, particlization, hadronic cascade

- **Hydro evolution:**  $\tau \leq \tau_{th}$   $T^{\mu\nu}(x) = T_{\text{free}}^{\mu\nu}(x)\mathcal{P}(\tau) + T_{\text{hyd}}^{\mu\nu}(x)(1 - \mathcal{P}(\tau)) \xrightarrow{\tau \geq \tau_{th}} T_{\text{hyd}}^{\mu\nu}(x)$   
 $= (\epsilon_{\text{hyd}}(x) + p_{\text{hyd}}(x) + \Pi)u_{\text{hyd}}^{\mu}(x)u_{\text{hyd}}^{\nu}(x) - (p_{\text{hyd}}(x) + \Pi)g^{\mu\nu} + \pi^{\mu\nu}.$

IC is the result of pre-thermal evolution reached at  $\tau_{th}$

**Solving of Israel-Stewart Relativistic Viscous Fluid Dynamics with  $\Pi=0$**

# The other stages: Hydro evolution, particlization, hadronic cascade

$$\tau \geq \tau_{th}$$

- Hydro evolution:**  $\tau \leq \tau_{th}$ 

$$T^{\mu\nu}(x) = T_{\text{free}}^{\mu\nu}(x)\mathcal{P}(\tau) + T_{\text{hyd}}^{\mu\nu}(x)(1 - \mathcal{P}(\tau)) \rightarrow T_{\text{hyd}}^{\mu\nu}(x)$$

$$= (\epsilon_{\text{hyd}}(x) + p_{\text{hyd}}(x) + \Pi)u_{\text{hyd}}^{\mu}(x)u_{\text{hyd}}^{\nu}(x) - (p_{\text{hyd}}(x) + \Pi)g^{\mu\nu} + \pi^{\mu\nu}.$$

## Solving of Israel-Stewart Relativistic Viscous Fluid Dynamics with $\Pi=0$

at the isotherm hypersurface  $T=165$  MeV

energy density  $\epsilon = 0.5$  GeV/fm<sup>3</sup> for the Laine-Schroeder EoS

Switching hypersurface build with help of Cornelius routine.

- Particlization:**

For particle distribution the Grad's 14 momentum ansatz is used:

$$\frac{d^3 \Delta N_i}{dp^* d(\cos\theta) d\phi} = \frac{\Delta\sigma_{\mu}^* p^{*\mu}}{p^{*0}} p^{*2} f_{eq}(p^{*0}; T, \mu_i) \left[ 1 + (1 \mp f_{eq}) \frac{p_{\mu}^* p_{\nu}^* \pi^{*\mu\nu}}{2T^2(\epsilon + p)} \right]$$

# The other stages: Hydro evolution, particlization, hadronic cascade

- Hydro evolution:**  $\tau \leq \tau_{th}$   $T^{\mu\nu}(x) = T_{\text{free}}^{\mu\nu}(x)\mathcal{P}(\tau) + T_{\text{hyd}}^{\mu\nu}(x)(1 - \mathcal{P}(\tau)) \xrightarrow{\tau \geq \tau_{th}} T_{\text{hyd}}^{\mu\nu}(x)$   
 $= (\epsilon_{\text{hyd}}(x) + p_{\text{hyd}}(x) + \Pi)u_{\text{hyd}}^{\mu}(x)u_{\text{hyd}}^{\nu}(x)$   
 $- (p_{\text{hyd}}(x) + \Pi)g^{\mu\nu} + \pi^{\mu\nu}.$

## Solving of Israel-Stewart Relativistic Viscous Fluid Dynamics with $\Pi=0$

- Particlization:** at the isotherm hypersurface  $T=165$  MeV  
energy density  $\epsilon = 0.5$  GeV/fm<sup>3</sup> for the Laine-Schroeder EoS  
Switching hypersurface build with help of Cornelius routine.

For particle distribution the Grad's 14 momentum ansatz is used:

$$\frac{d^3 \Delta N_i}{dp^* d(\cos\theta) d\phi} = \frac{\Delta \sigma_{\mu}^* p^{*\mu}}{p^{*0}} p^{*2} f_{eq}(p^{*0}; T, \mu_i) \left[ 1 + (1 \mp f_{eq}) \frac{p_{\mu}^* p_{\nu}^* \pi^{*\mu\nu}}{2T^2(\epsilon + p)} \right]$$

- Hadronic cascade:** The above distribution function with Poisson distributions for each sort of particle numbers is the input for UrQMD cascade.

# The other stages: Hydro evolution, particlization, hadronic cascade

$$\tau \geq \tau_{th}$$

- Hydro evolution:**  $\tau \leq \tau_{th}$ 

$$T^{\mu\nu}(x) = T_{\text{free}}^{\mu\nu}(x)\mathcal{P}(\tau) + T_{\text{hyd}}^{\mu\nu}(x)(1 - \mathcal{P}(\tau)) = T_{\text{hyd}}^{\mu\nu}(x)$$

$$= (\epsilon_{\text{hyd}}(x) + p_{\text{hyd}}(x) + \Pi)u_{\text{hyd}}^{\mu}(x)u_{\text{hyd}}^{\nu}(x)$$

$$- (p_{\text{hyd}}(x) + \Pi)g^{\mu\nu} + \pi^{\mu\nu}.$$

## Solving of Israel-Stewart Relativistic Viscous Fluid Dynamics with $\Pi = 0$

- Particlization:**

at the isotherm hypersurface  $T=165$  MeV

energy density  $\epsilon = 0.5$  GeV/fm<sup>3</sup> for the Laine-Schroeder EoS

Switching hypersurface build with help of Cornelius routine.

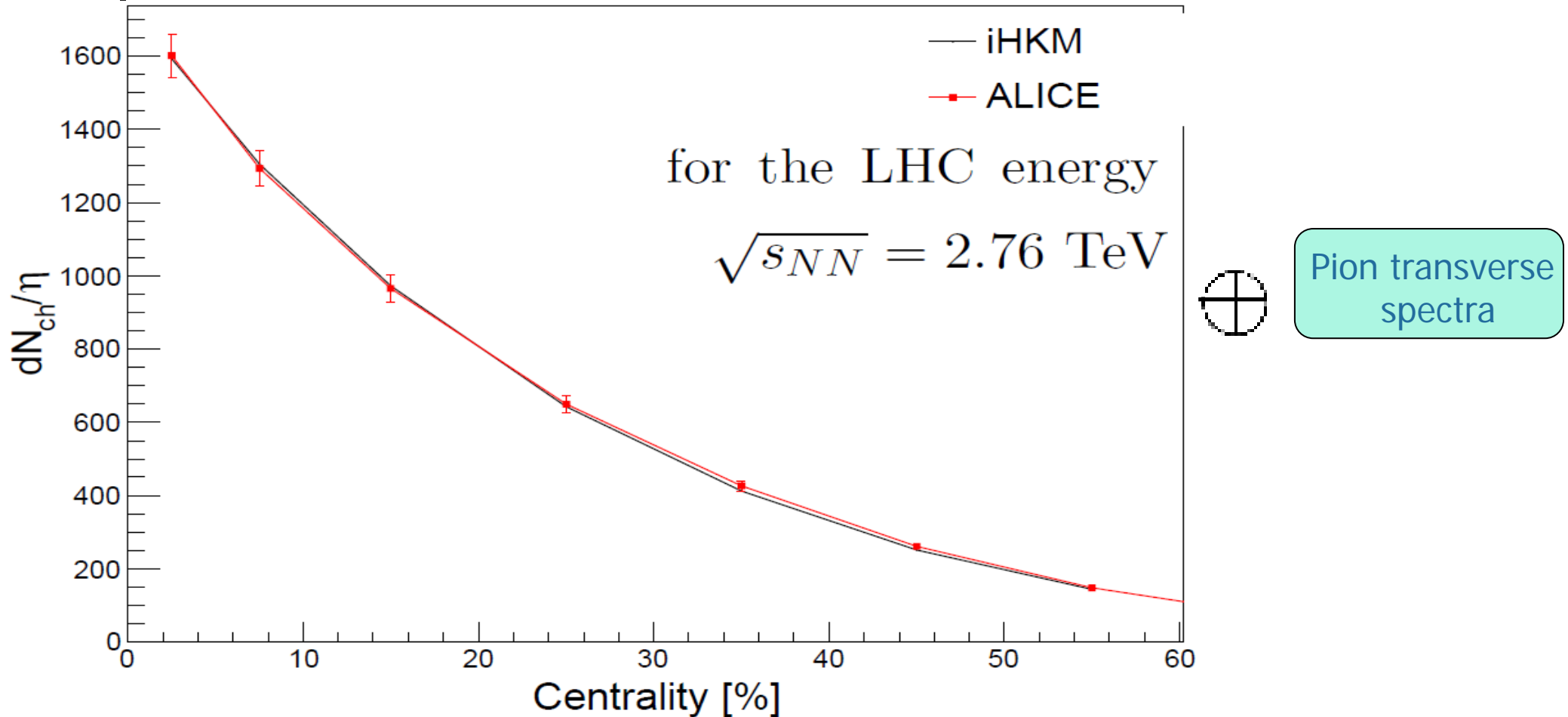
For particle distribution  
the Grad's 14  
momentum ansatz is  
used:

$$\frac{d^3 \Delta N_i}{dp^* d(\cos\theta) d\phi} = \frac{\Delta \sigma_{\mu}^* p^{*\mu}}{p^{*0}} p^{*2} f_{eq}(p^{*0}; T, \mu_i) \left[ 1 + (1 \mp f_{eq}) \frac{p_{\mu}^* p_{\nu}^* \pi^{*\mu\nu}}{2T^2(\epsilon + p)} \right]$$

- Hadronic cascade:** The above distribution function with Poisson distributions for each sort of particle numbers is the input for UrQMD

Details are in: Naboka, Karpenko, Yu.S. C **93** (2016) 024902

# Multiplicity dependence of all charged particles on centrality



parameter values:  $\alpha = 0.24, \tau_{th} = 1\text{fm}/c, \epsilon_0 = f(\tau_0, \tau_{rel}, \eta/s, \Lambda, \text{EoS} \rightarrow T_{ch} \approx T_h)$

# The iHKM parameters at Laine-Shroeder EoS

The  $\frac{dN_{ch}}{d\eta}(c)$  is OK at fixed relative contribution of binary collision  $\alpha = 0.24$ .

but at different max initial energy densities  
when other parameters change:

The two values of the shear viscosity  
to entropy is used for comparison:

$$\eta/s = 0.08 \approx \frac{1}{4\pi} \text{ and } \eta/s = 0.2$$

The basic result (selected by red) is  
compared with results at other  
parameters, including viscous and ideal  
pure thermodynamic scenarios  
(starting at  $\tau_0$  without pre-thermal stage  
but with subsequent hadronic cascade).

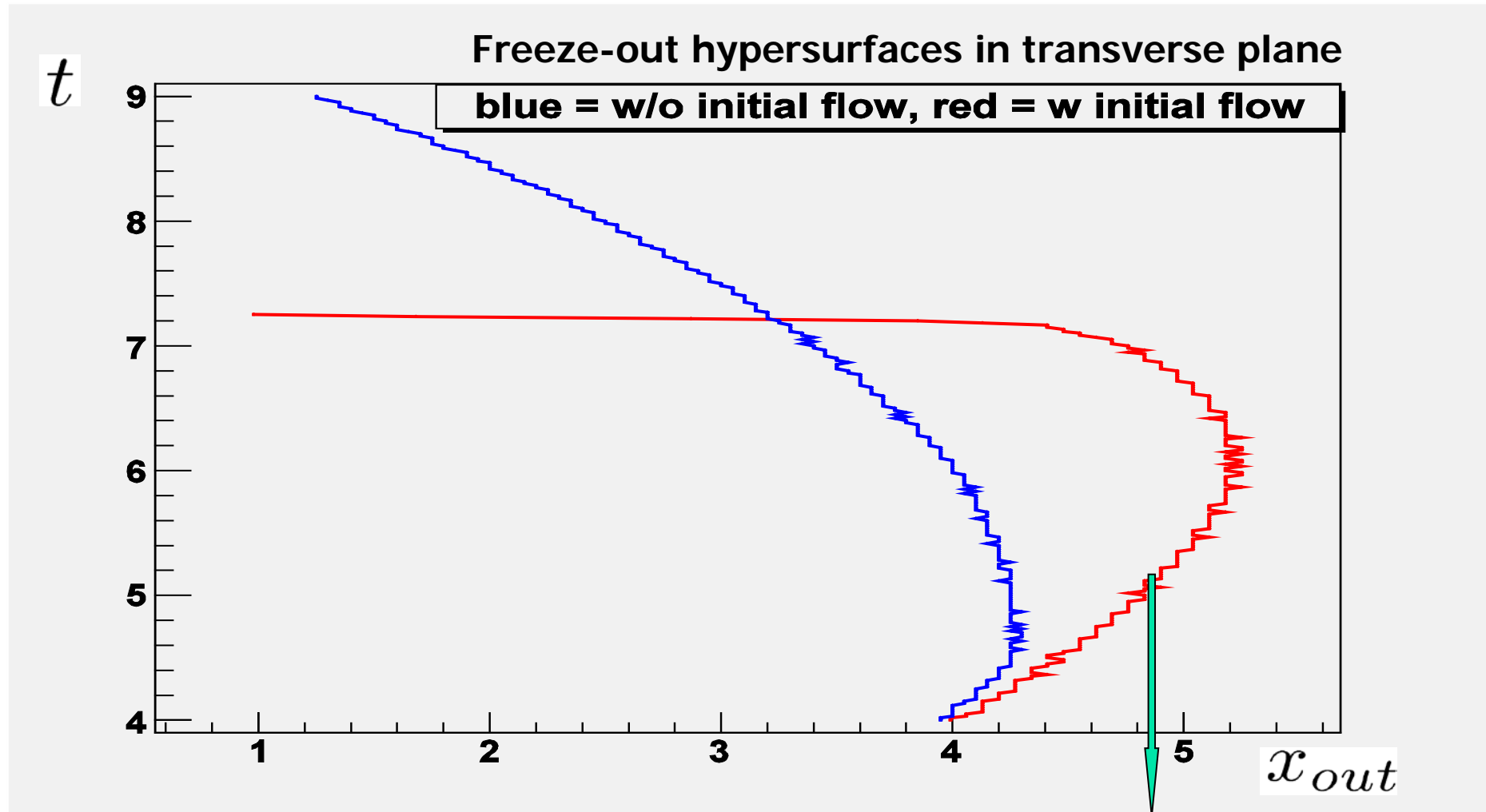
Model	$\Lambda$	$\tau_{rel}$	$\eta/S$	$\tau_0$	$\langle \frac{\chi^2}{ndf} \rangle$	$\epsilon_0$ (GeV/fm <sup>3</sup> )
Hydro			0	0.1	5.16	1076.5
Hydro			0.08	0.1	6.93	738.8
iHKM	1	0.25	0.08	0.1	3.35	799.5
iHKM	100	0.25	0.08	0.1	3.28	678.8
iHKM	100	0.75	0.08	0.1	3.52	616.5
iHKM	100	0.25	0.2	0.1	6.61	596.9
iHKM	100	0.25	0.08	0.5	5.36	126.7

The values  $\tau_0, \tau_{rel}$  correspond to fm/c.

No dramatic worsening of the results  
happens if simultaneously with changing  
of parameters/scenarios renormalize maximal  
initial energy density.

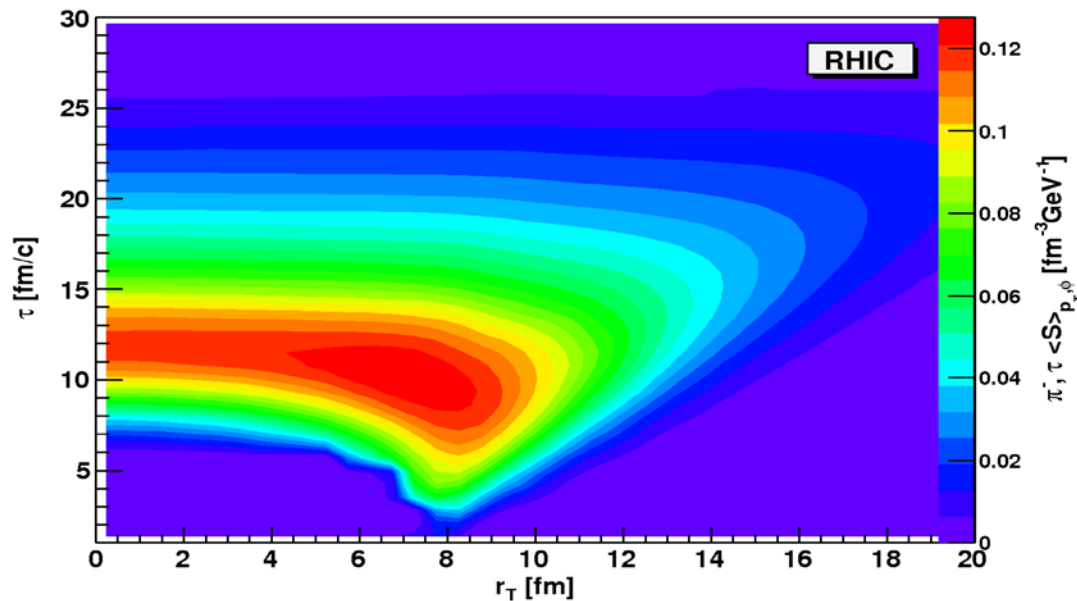
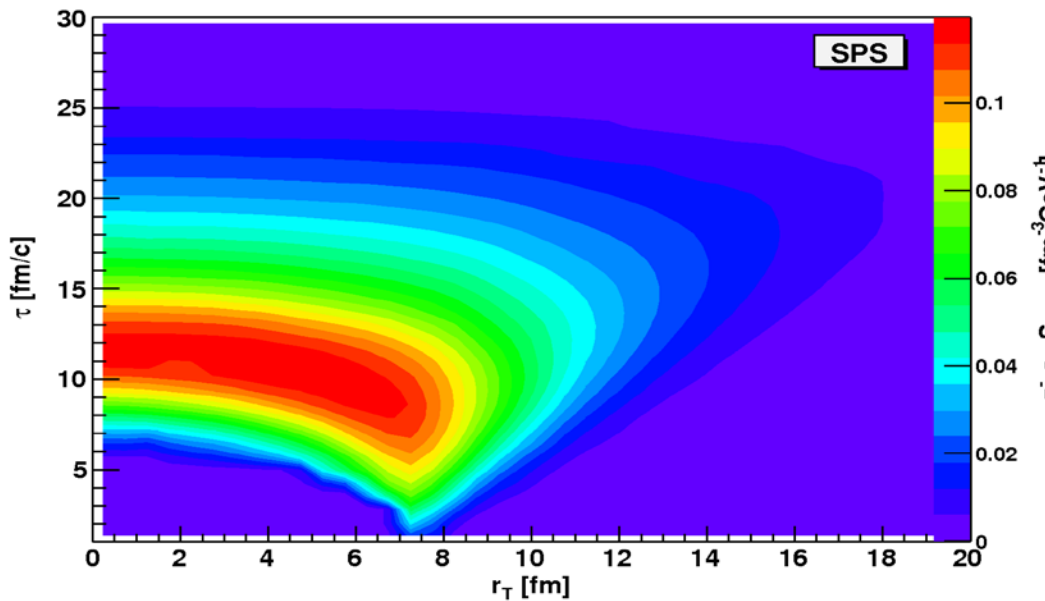


A few principal results from HKM/iHKM on the  
correlation femtoscopy

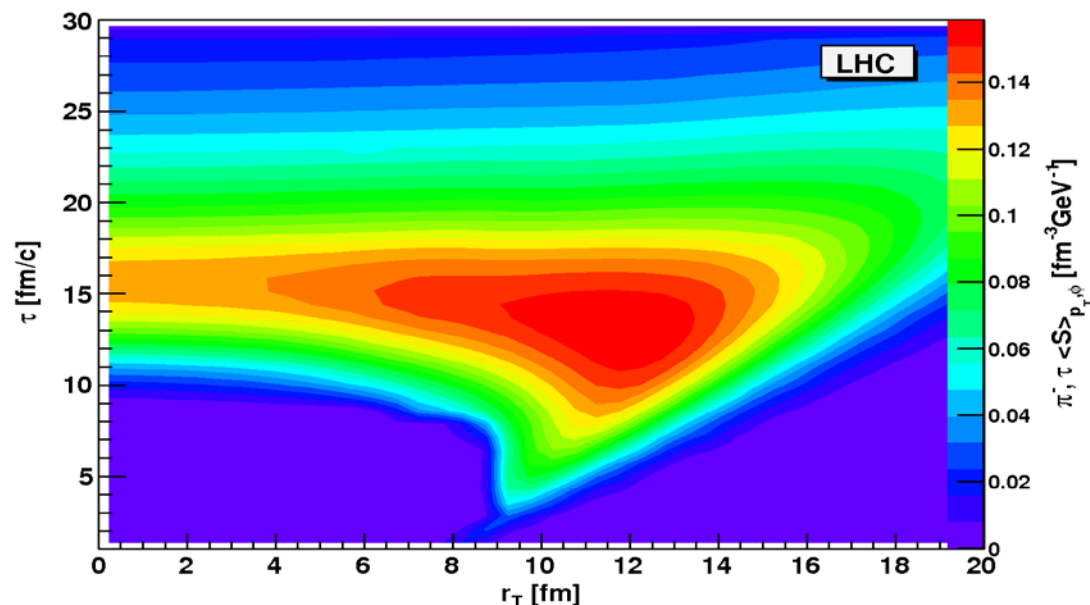


$$R_{out}^2 \approx R_{side}^2 + v^2 \langle \Delta t^2 \rangle_p - 2v \langle \Delta x_{out} \Delta t \rangle_p, v = \frac{p_T}{p_0}$$

# Emission functions for top SPS, RHIC and LHC energies



$$R_{out}^2 \approx R_{side}^2 + v^2 \langle \Delta t^2 \rangle_p - 2v \langle \Delta x_{out} \Delta t \rangle_p, v = \frac{p_T}{p^0}$$



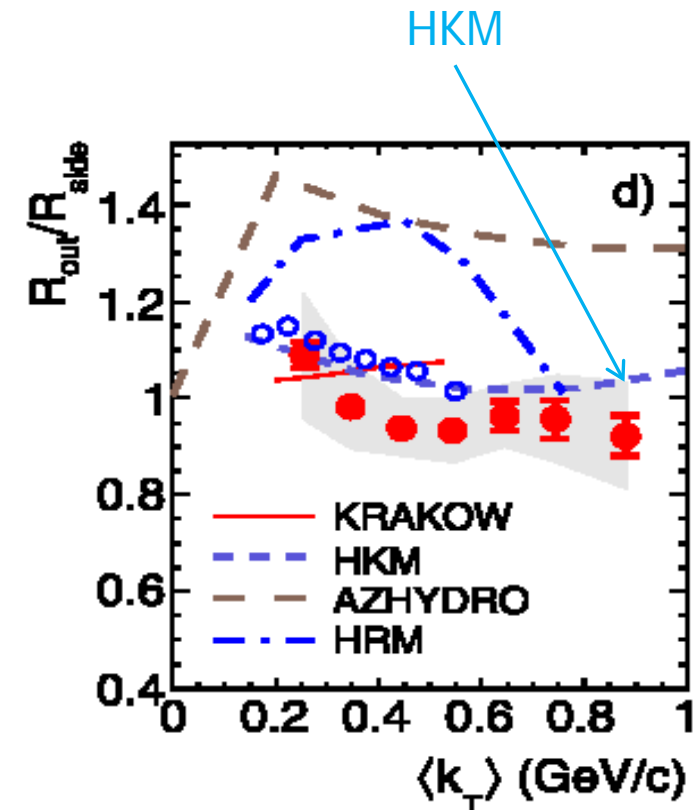
# HKM prediction: solution of the HBT Puzzle

Two-pion Bose–Einstein correlations in central Pb–Pb collisions  
at  $\sqrt{s_{NN}} = 2.76$  TeV<sup>☆</sup> ALICE Collaboration Physics Letters B 696 (2011) 328.



## Quotations:

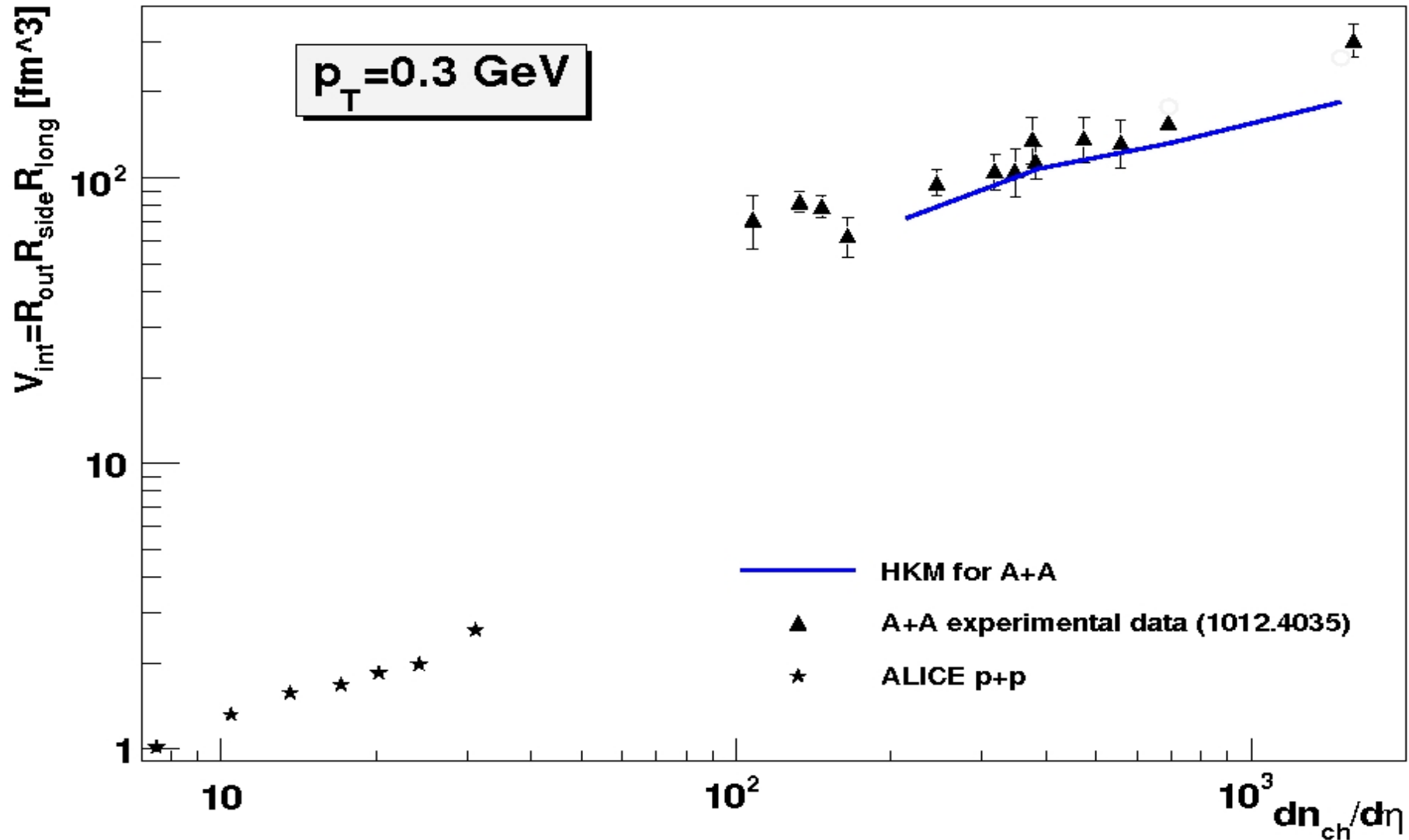
Available model predictions are compared to the experimental data in Figs. 2-d and 3. Calculations from three models incorporating a hydrodynamic approach, AZHYDRO [45], KRAKOW [46,47], and HKM [48,49], and from the hadronic-kinematics-based model HRM [50,51] are shown. An in-depth discussion is beyond the scope of this Letter but we notice that, while the increase of the radii between RHIC and the LHC is roughly reproduced by all four calculations, only two of them (KRAKOW and HKM) are able to describe the experimental  $R_{out}/R_{side}$  ratio.



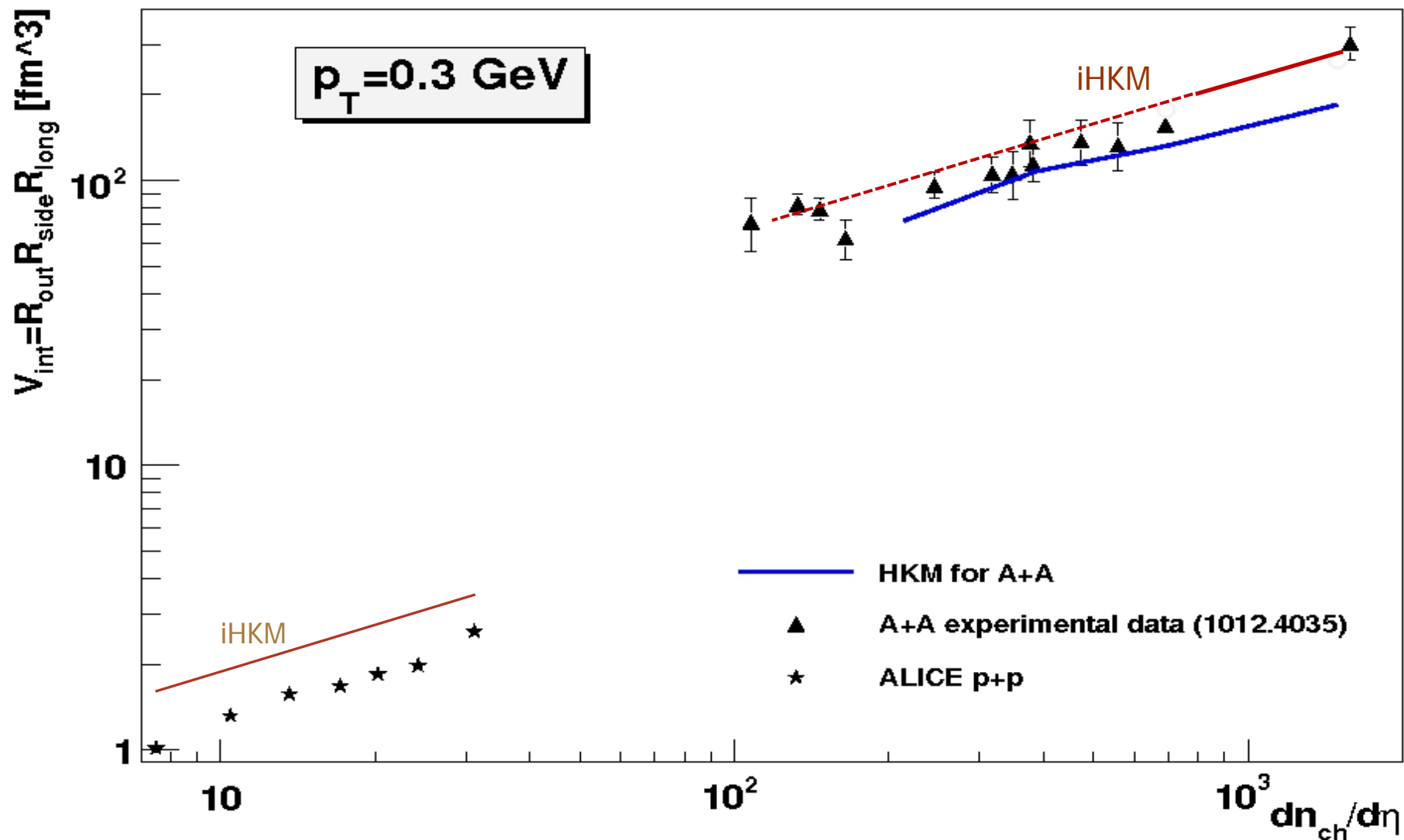
[48] I.A. Karpenko, Y.M. Sinyukov, Phys. Lett. B 688 (2010) 50.

[49] N. Armesto, et al. (Eds.), J. Phys. G 35 (2008) 054001.

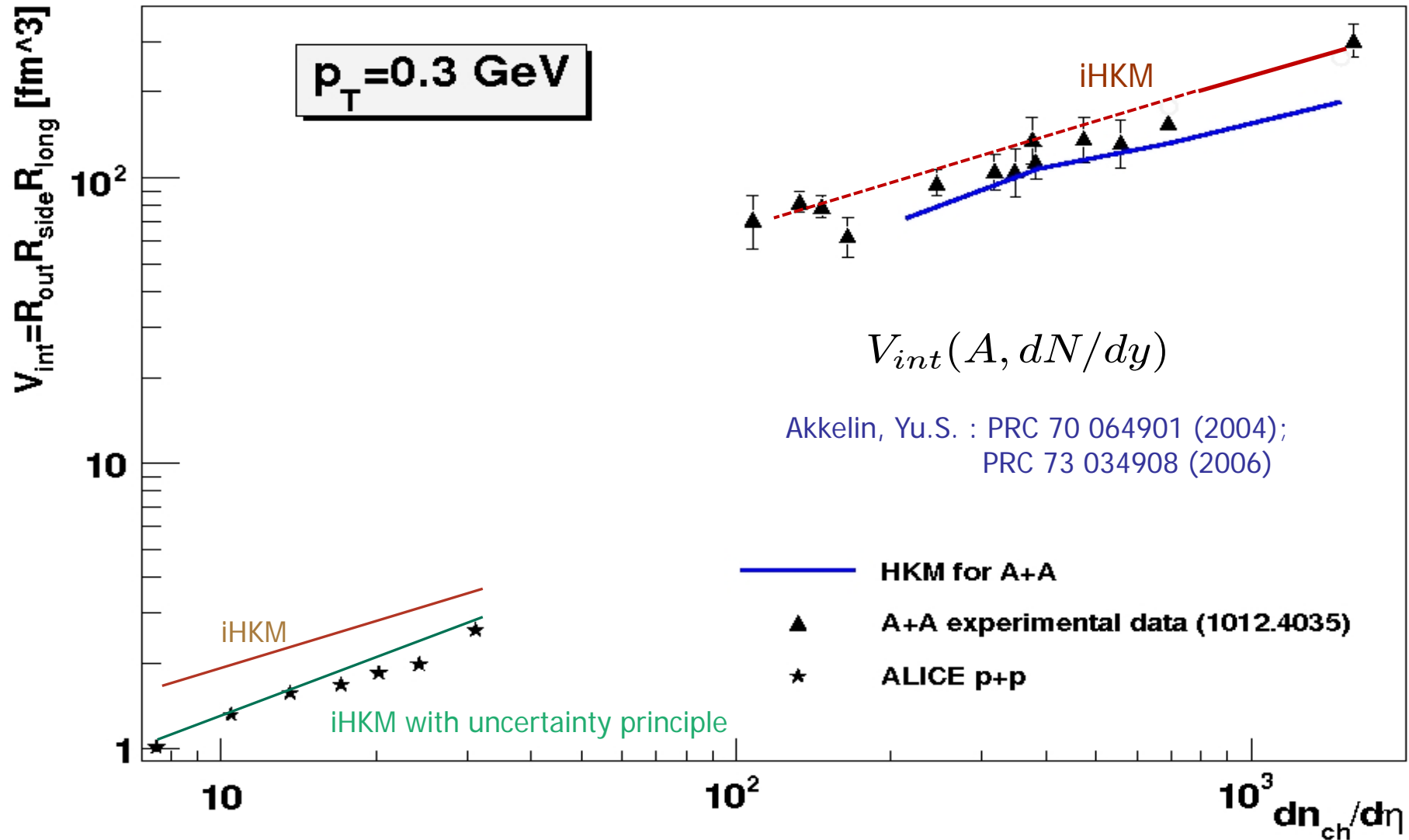
# Interferometry volume $V_{int}$ in LHC p-p and **central** Au-Au, Pb-Pb collisions



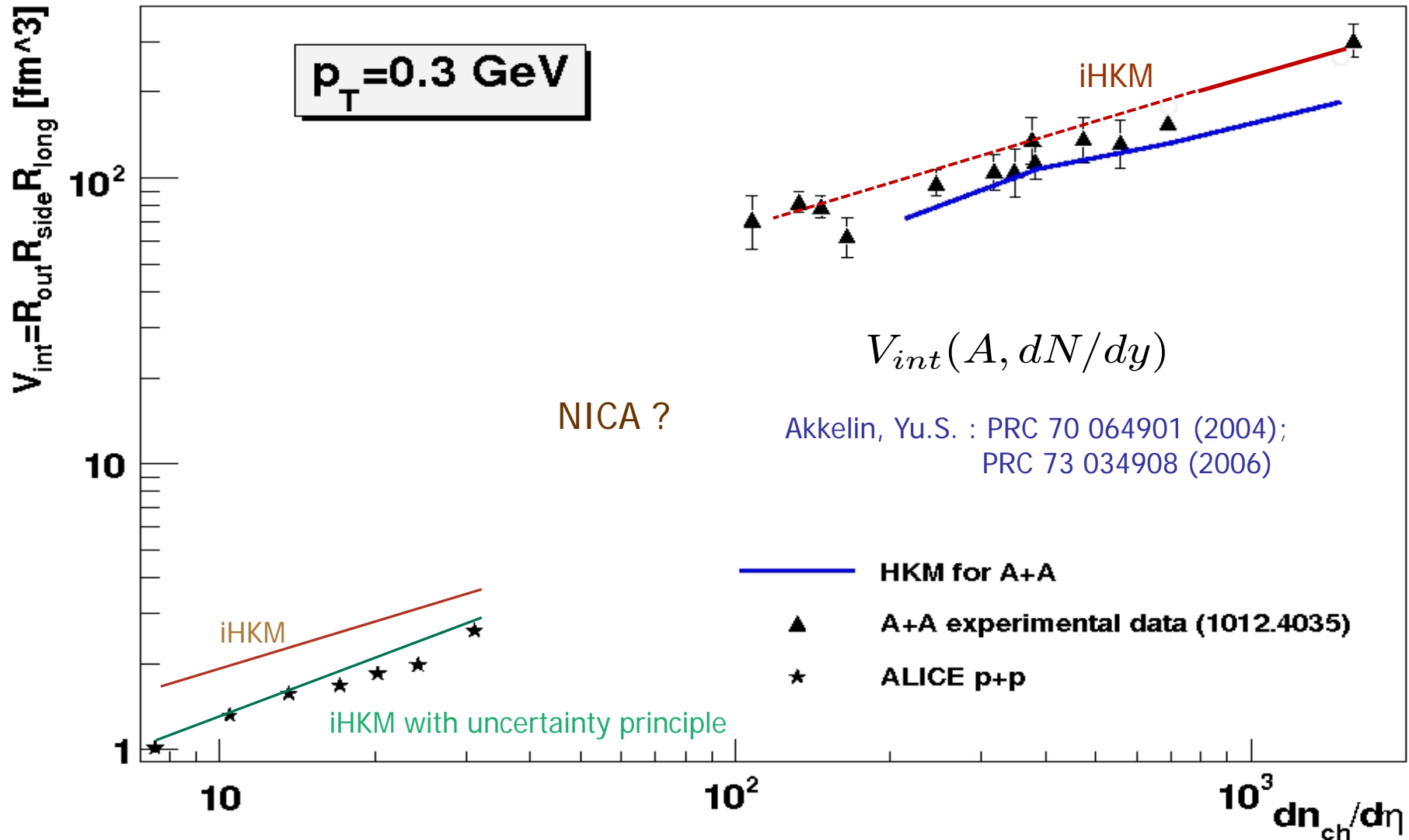
# Interferometry volume $V_{int}$ in LHC p-p and **central** Au-Au, Pb-Pb collisions



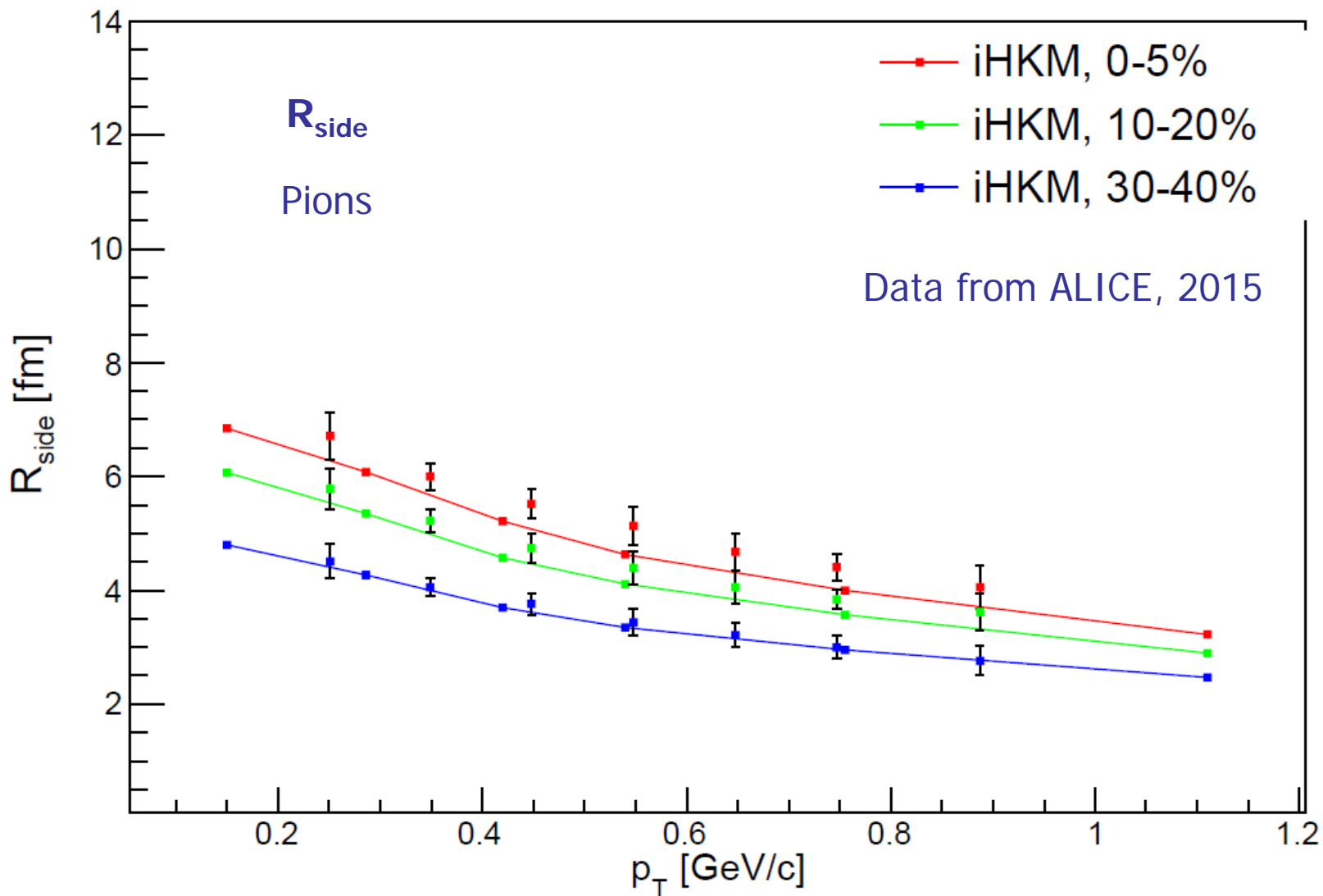
# Interferometry volume $V_{int}$ in LHC p-p and **central** Au-Au, Pb-Pb collisions



# Interferometry volume $V_{int}$ in LHC p-p and **central** Au-Au, Pb-Pb collisions

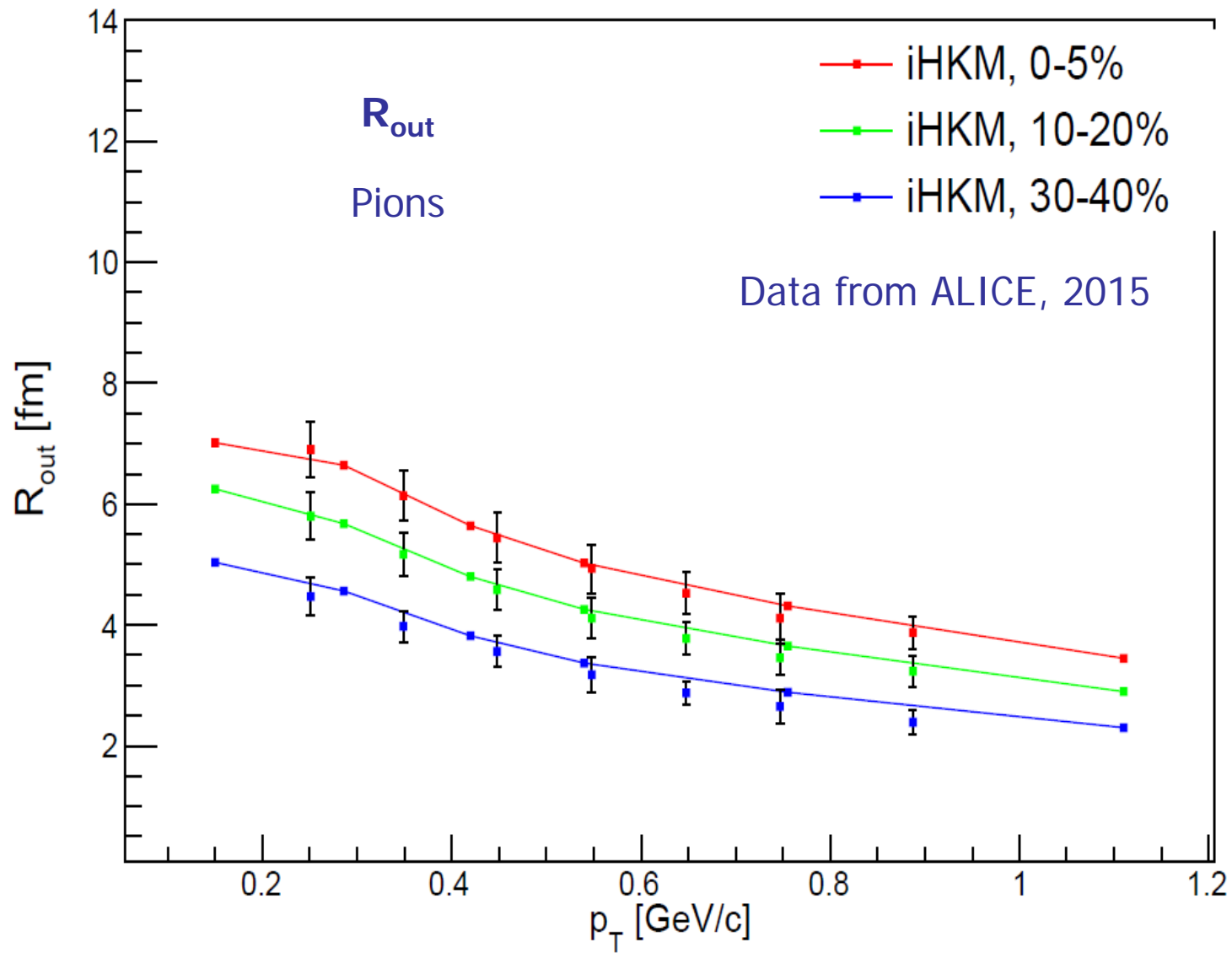




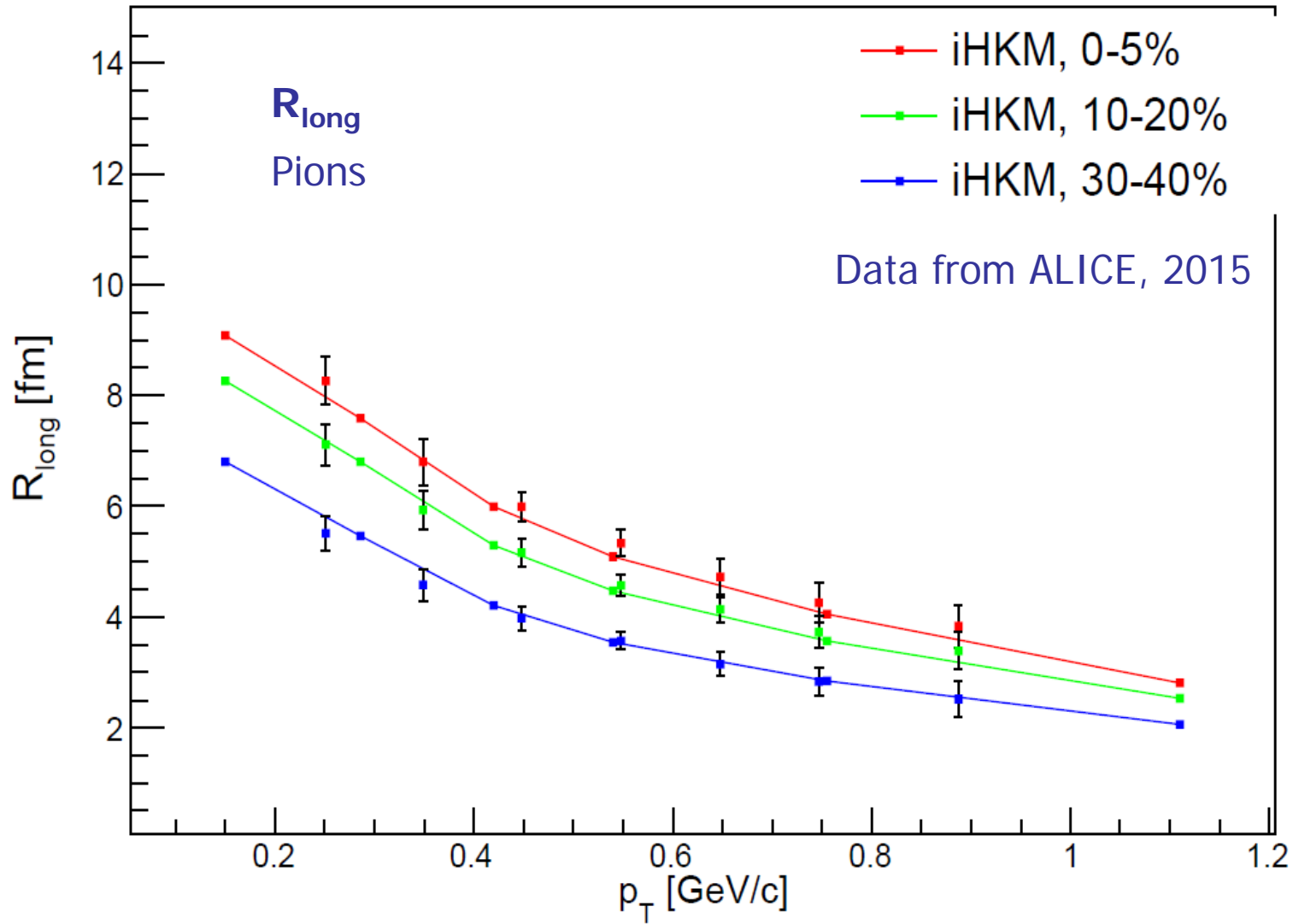


The  $R_{side}$  dependence on transverse momentum for different centralities in the iHKM

scenario under the same conditions as in Fig. 1. The experimental data are from [33].

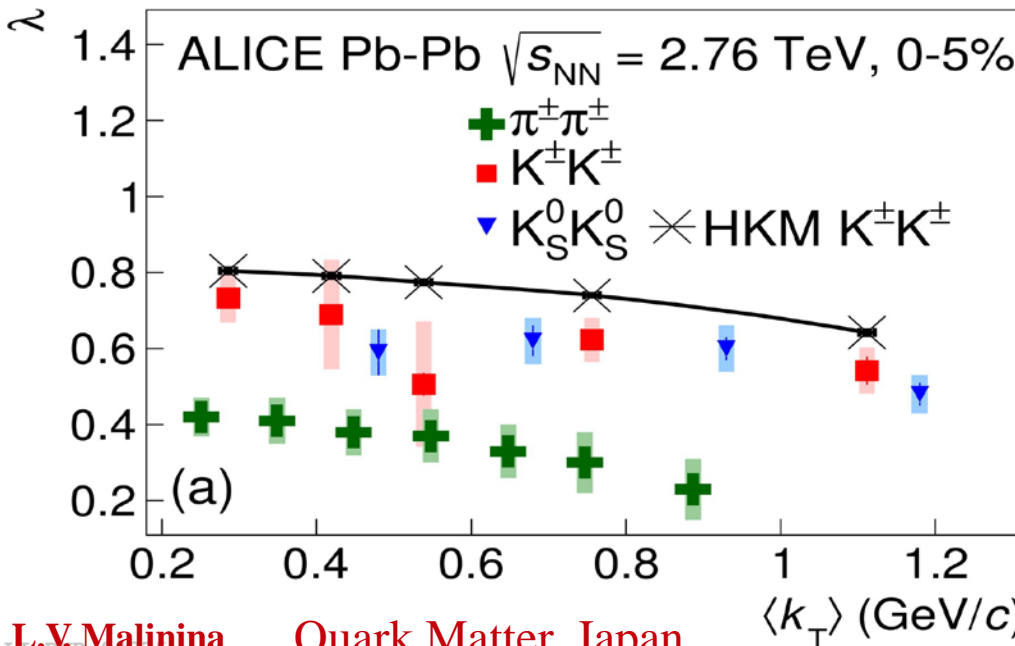
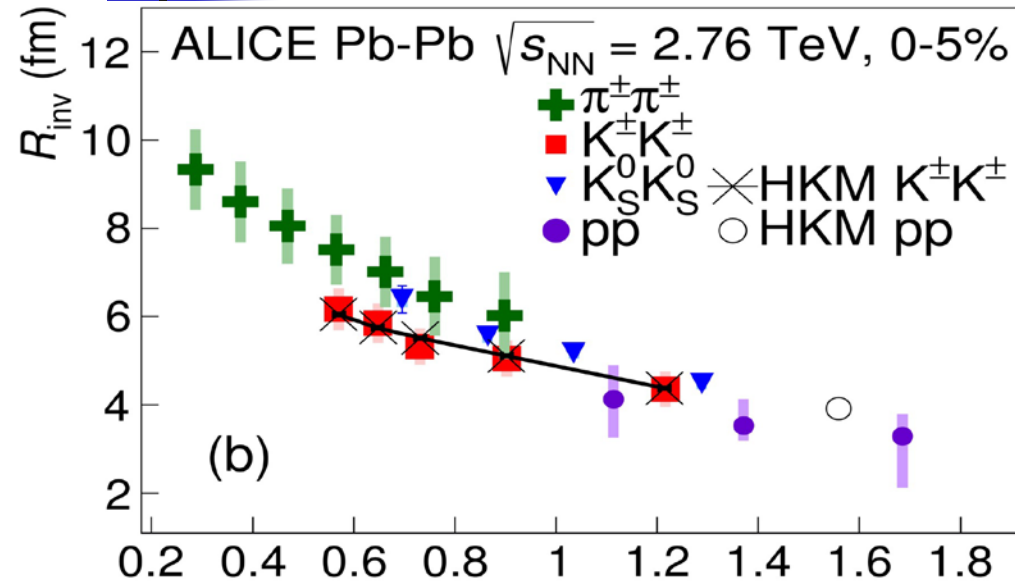


The  $R_{out}$  dependence on transverse momentum for different centralities in the iHKM basic scenario under the same conditions as in Fig. 1.



The  $R_{long}$  dependence on transverse momentum for different centralities in the iHKM basic scenario - the same conditions as in Fig. 1. The experimental data are from [33].

# $K^\pm K^\pm$ and $K^0 K^0$ in Pb-Pb: HKM model



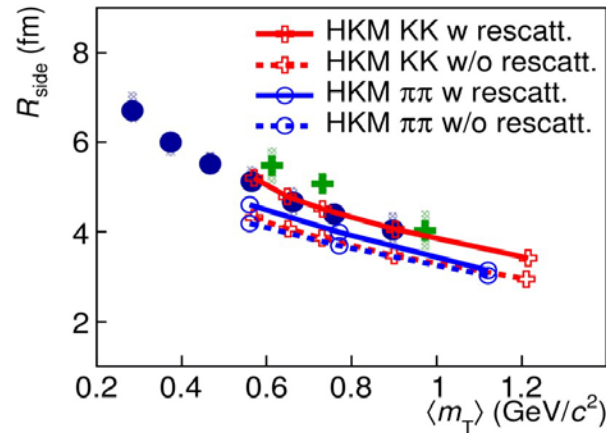
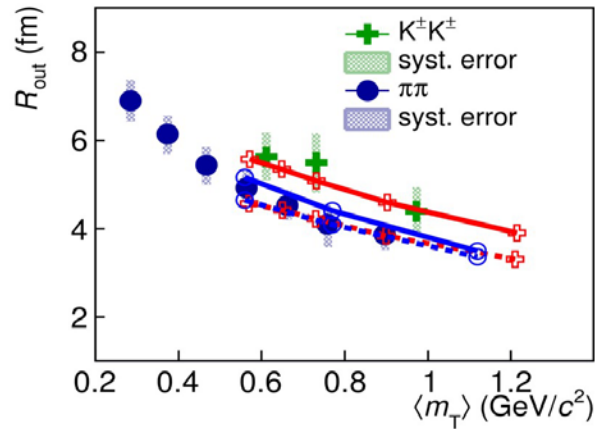
*New results from [ArXiv.org:1506.07884](https://arxiv.org/abs/1506.07884)*

- R and  $\lambda$  for  $\pi^\pm \pi^\pm$ ,  $K^\pm K^\pm$ ,  $K^0 K^0$ , pp for 0-5% centrality
- Radii for kaons show good agreement with HKM predictions for  $K^\pm K^\pm$  (V. Shapoval, P. Braun-Munzinger, Yu. Sinyukov Nucl.Phys.A929 (2014))

- $\lambda$  decrease with  $k_T$ , both data and HKM
- HKM prediction for  $\lambda$  slightly overpredicts the data
- $\Lambda_\pi$  are lower  $\Lambda_K$  due to the stronger influence of resonances

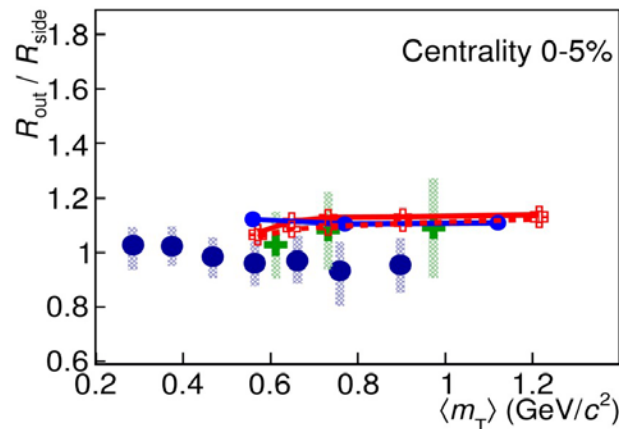
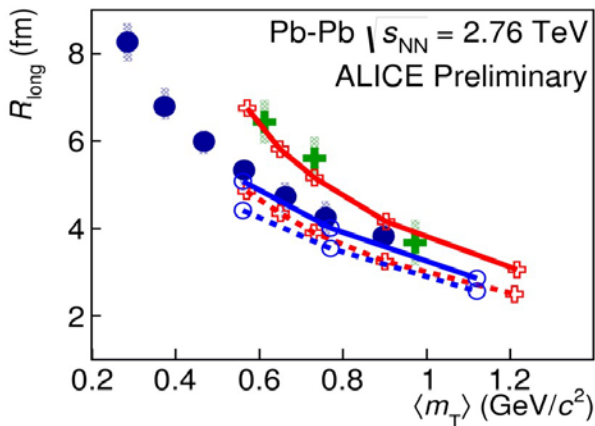
ALICE Coll. Phys. Rev. C 96 ... (2017)

# Comparison with HKM for 0-5% centrality



- HKM model with re-scatterings (M. Shapoval, P. Braun-Munzinger, Iu.A. Karpenko, Yu.M. Sinyukov, Nucl.Phys. A 929 (2014) 1.) describes well ALICE  $\pi$  & K data.

● HKM model w/o re-scatterings demonstrates



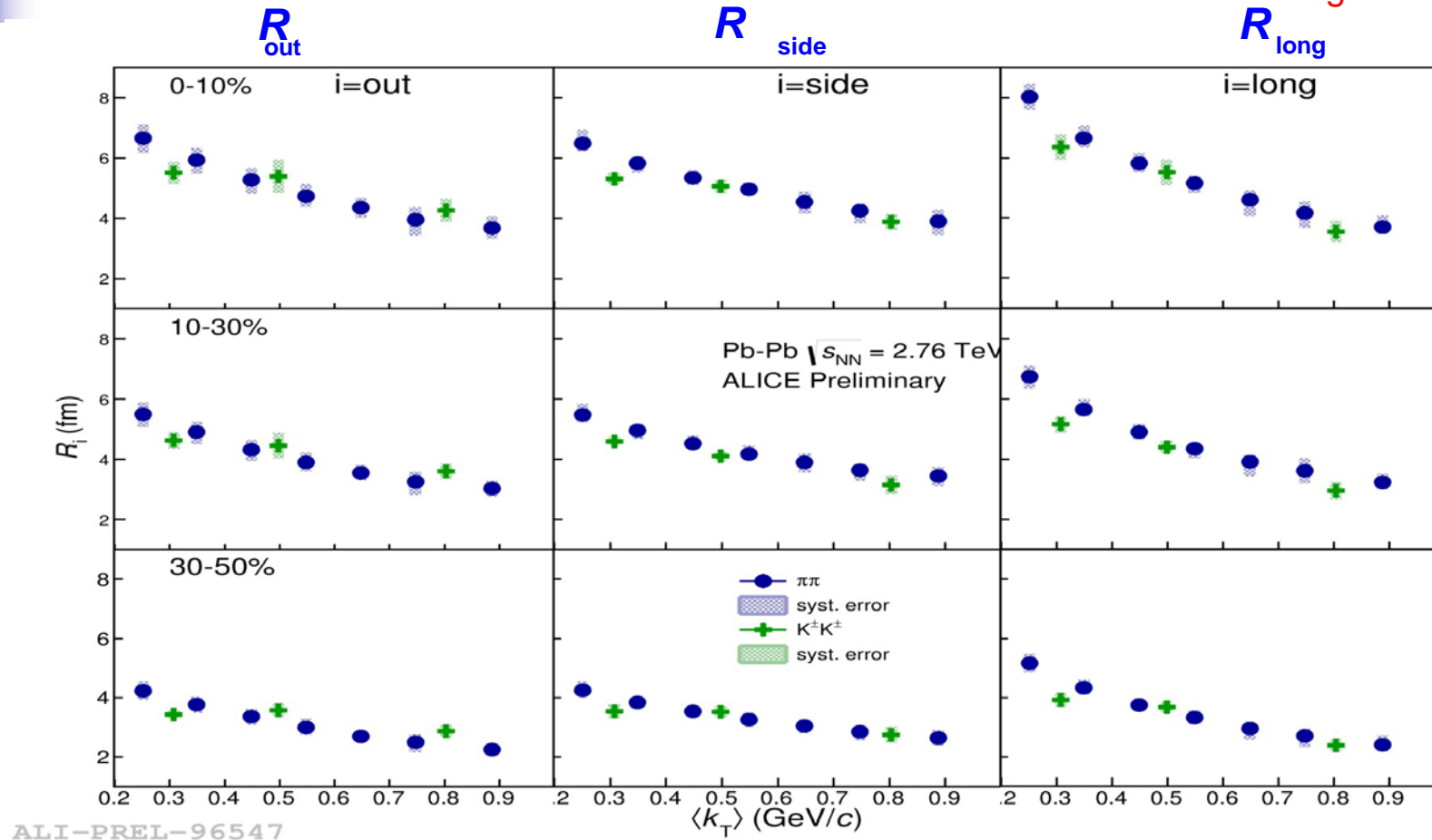
● approximate  $m_T$  scaling for  $\pi$  & K, but does not describe ALICE  $\pi$  & K data

- The observed deviation from  $m_T$  scaling is explained in (M. Shapoval, P. Braun-Munzinger, Iu.A. Karpenko, Yu.M. Sinyukov, Nucl.Phys. A 929 (2014) 1.) by essential transverse flow & re-scattering phase.

● HKM model slightly underestimates  $R_{\text{side}}$  and overestimates  $R_{\text{out}} / R_{\text{side}}$  ratio for  $\pi$

# 3D $K^\pm K^\pm$ & $\pi\pi$ radii versus $k_T$

Pion results from [ArXiv.org:1507.06842](https://arxiv.org/abs/1507.06842)



ALI-PREL-96547

- Radii scale better with  $k_T$  than with  $m_T$  according with HKM predictions  
(V. Shapoval, P. Braun-Munzinger, Iu.A. Karpenko, Yu.M. Sinyukov, Nucl.Phys. A 929 (2014) 1);
- Similar observations were reported by PHENIX at RHIC ([arxiv:1504.05168](https://arxiv.org/abs/1504.05168)).

# Space-time picture of the pion and kaon emission

$$R_l^2(k_T) = \underbrace{\tau^2 \lambda^2 \left(1 + \frac{3}{2} \lambda^2\right)}_{2015} \approx \text{w/o transv. expansion} \approx \underbrace{\tau^2 \frac{T}{m_T}}_{1987} \underbrace{\frac{K_2\left(\frac{m_T}{T}\right)}{K_1\left(\frac{m_T}{T}\right)}}_{1995}$$

where

$$\lambda^2 = \frac{T}{m_T} \left(1 - \frac{\overbrace{k_T^2}^{\bar{v}_T^2}}{(m_T + \alpha T)^2}\right)^{1/2}$$

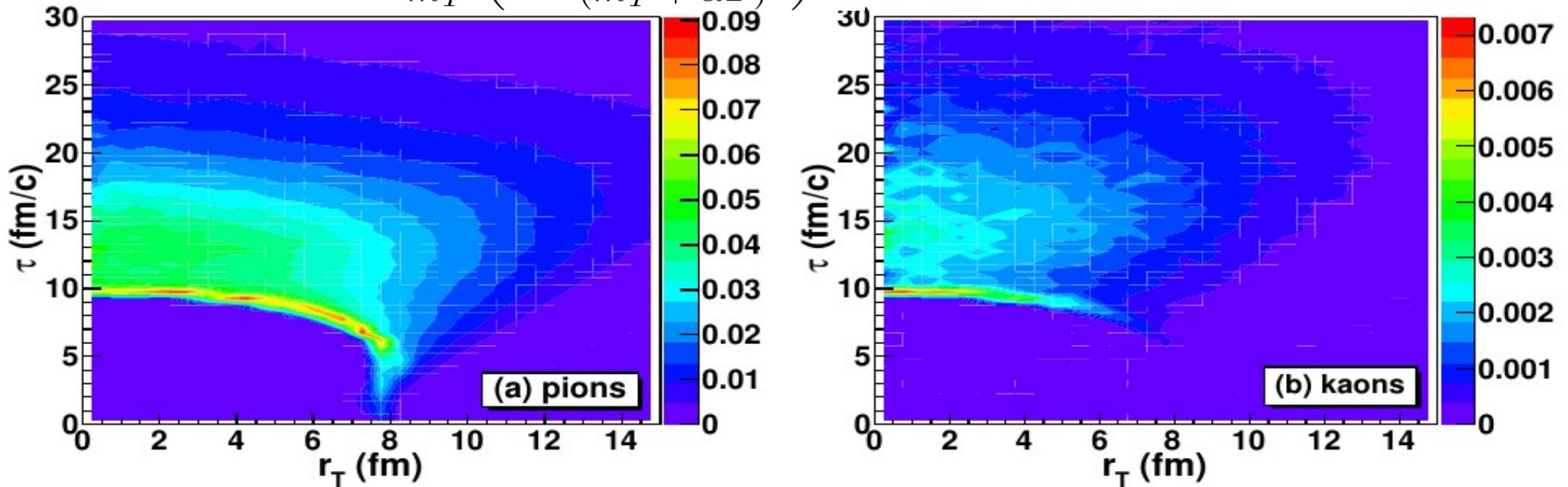


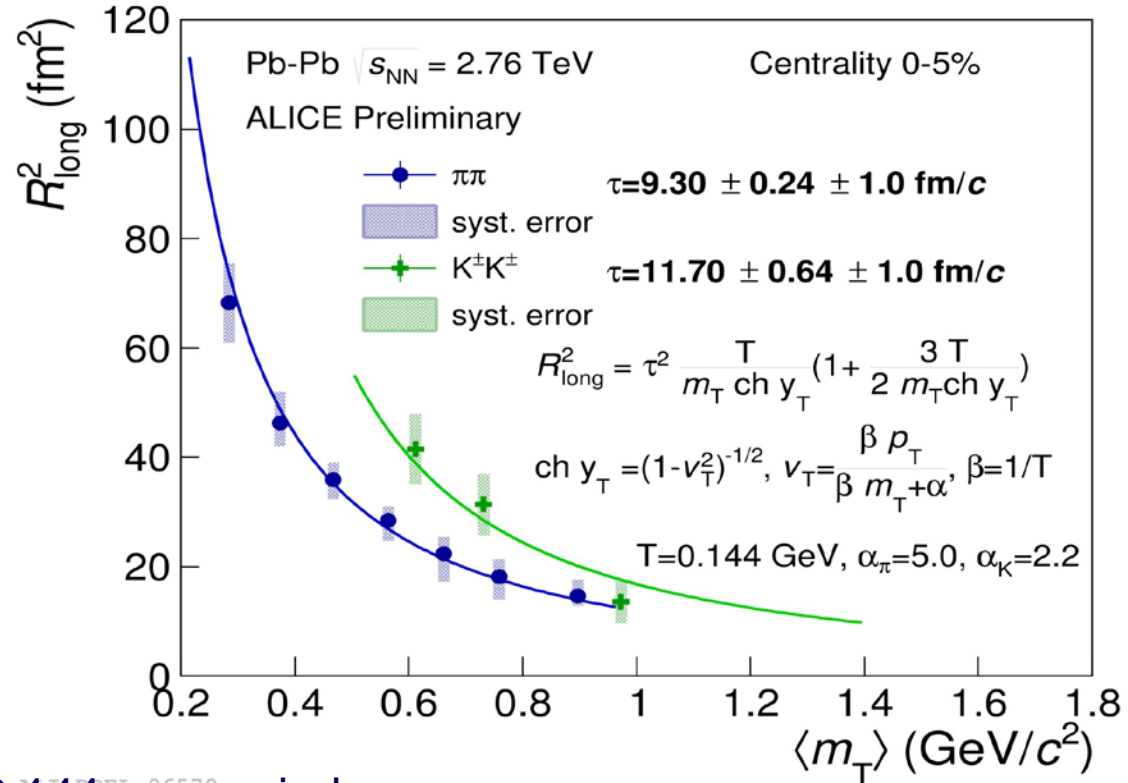
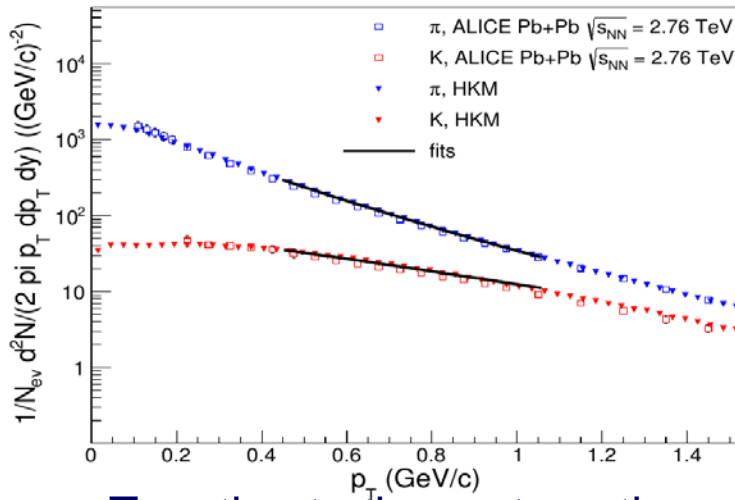
FIG. 4. The momentum angle averaged emission functions per units of space-time and momentum rapidities  $g(\tau, r_T, p_T)$  [ $\text{fm}^{-3}$ ] (see body text) for pions (a) and kaons (b) obtained from the HKM simulations of Pb+Pb collisions at the LHC  $\sqrt{s_{NN}} = 2.76$  GeV,  $0.2 < p_T < 0.3$  GeV/c,  $|y| < 0.5$ ,  $e = 0 - 5\%$ . From Yu.S., Shapoval, Naboka, Nucl. Phys. A 946 (2016) 247 ([arXiv:1508.01812](https://arxiv.org/abs/1508.01812))

# Extraction of emission time from fit $R_{\text{long}}$



- The new formula for extraction of the maximal emission time for the case of strong transverse flow was used ( Yu. S., Shapoval, Naboka, Nucl. Phys. A 946 (2016) 227 )

- The parameters of freeze-out:  $T$  and “intensity of transverse flow”  $\alpha$  were fixed by fitting  $\pi$  and  $K$  spectra ( arxiv:1508.01812 )

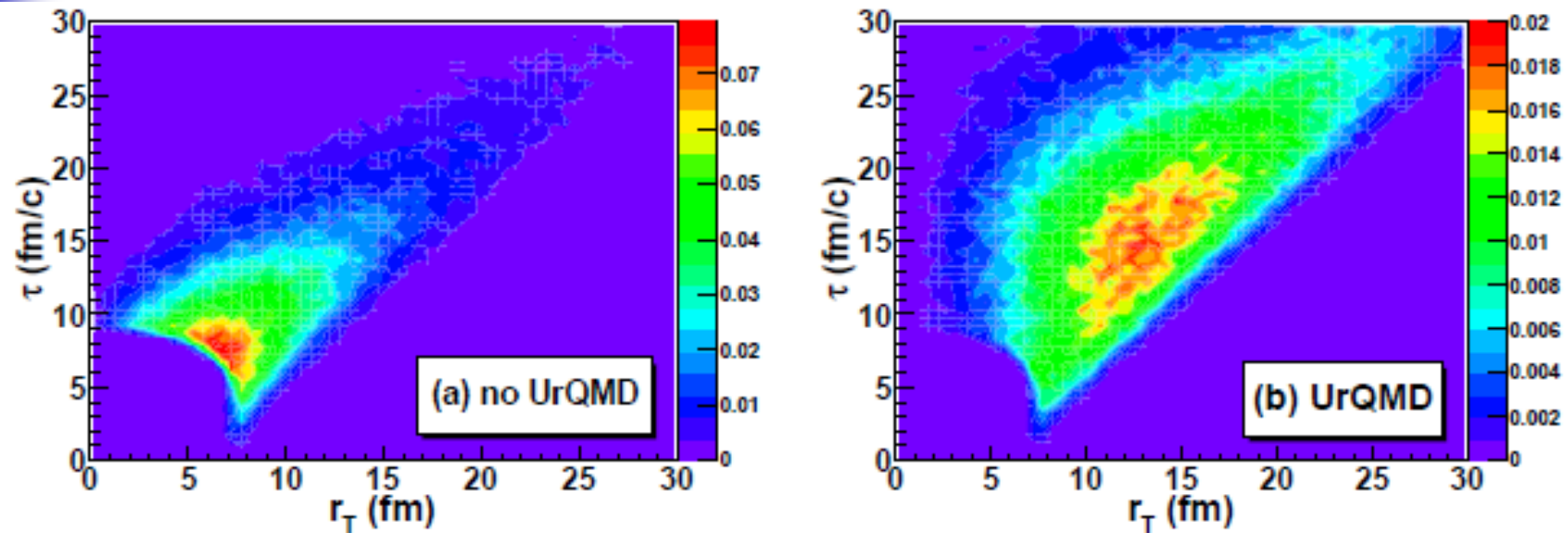


- To estimate the systematic errors:  $T = 0.144$  was varied on  $\pm 0.03$  GeV & free  $\alpha_{\pi}, \alpha_K$  were used; systematic errors  $\sim 1$  fm/c
- Indication:  $\tau_{\pi} < \tau_K$ . Possible explanations ( arxiv:1508.01812 ): HKM includes re-scatterings (UrQMD cascade): e.g.  $K\pi \rightarrow K^*(892) \rightarrow K\pi$ ,  $KN \rightarrow K^*(892)X$ ; ( $K^*(892)$  lifetime 4-5 fm/c) [ $\pi N \rightarrow N^*(\Delta)X$ ,  $N^*(\Delta) \rightarrow \pi X$  ( $N^*$ 's ( $\Delta$ s)- short lifetime)]



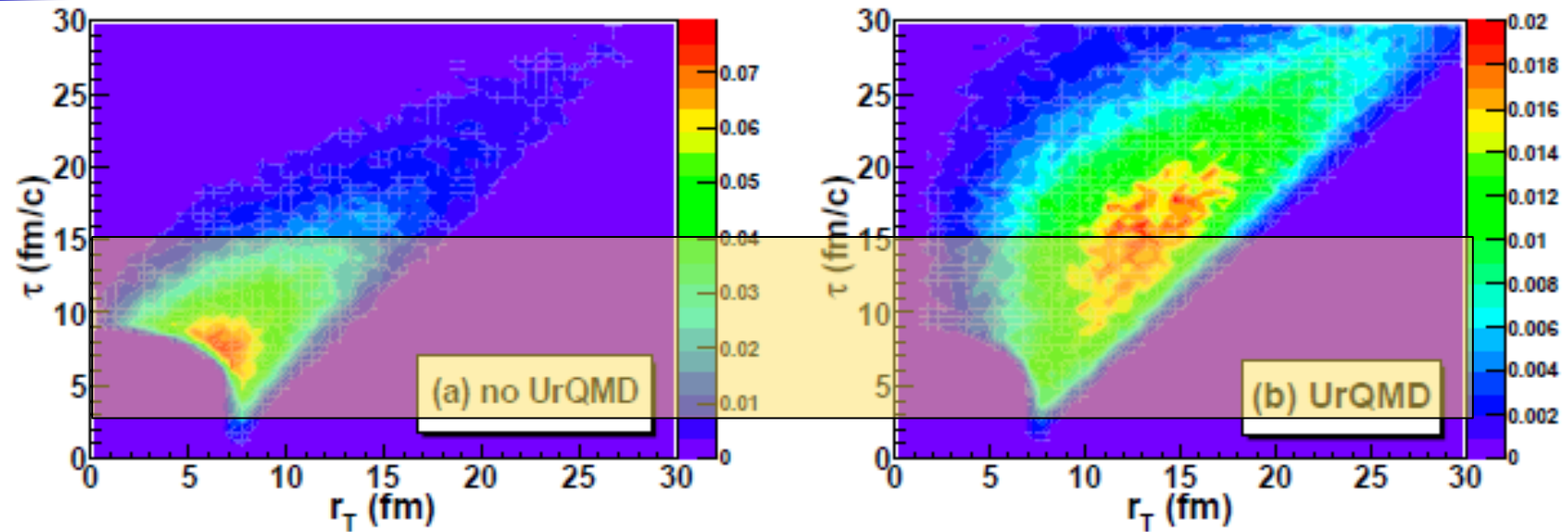
# $K^*$ probes

$K^*(892)$  life time is 4.2 fm/c



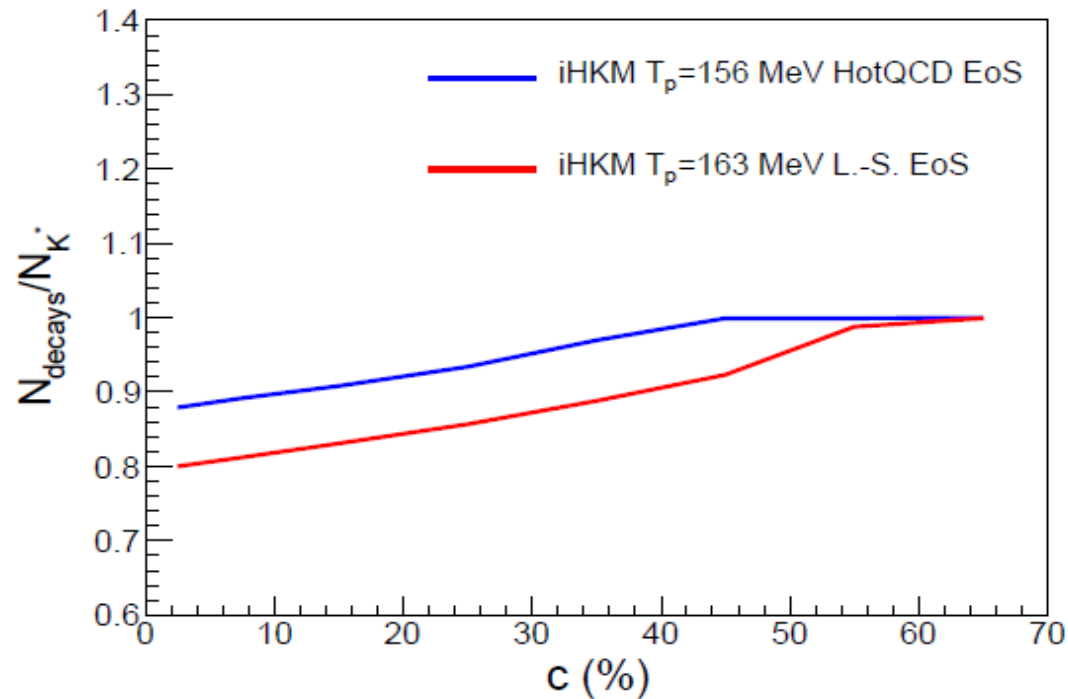
The comparison of the emission functions  $g(\tau, r_T)$ , averaged over complementary space and momentum components, of  $K^+\pi^-$  pairs, associated with  $K(892)^{*0}$  decay products, for two cases: (a) free-streaming of the particles and resonances, and (b) UrQMD hadron cascade. The plots are obtained using iHKM simulations of Pb+Pb collisions at the LHC  $\sqrt{s_{NN}} = 2.76$  GeV,  $0.3 < k_T < 5$  GeV/c,  $|y| < 0.5$ ,  $c = 5 - 10\%$ .

$K^{*0} \rightarrow K^+\pi^-$  radiation picture in iHKM.  
Sudden vs continuous thermal freeze-out at the LHC.



Less than 30% of direct  $K^*$  can be seen till 15 fm/c

# Suppression of $K^{*0}$ due to continuous thermal freeze-out (LHC)



70% - 20% = 50%  
Therefore  
at least 50% of direct  $K^{*0}$  are  
recreated in reactions:

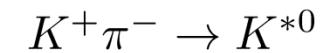
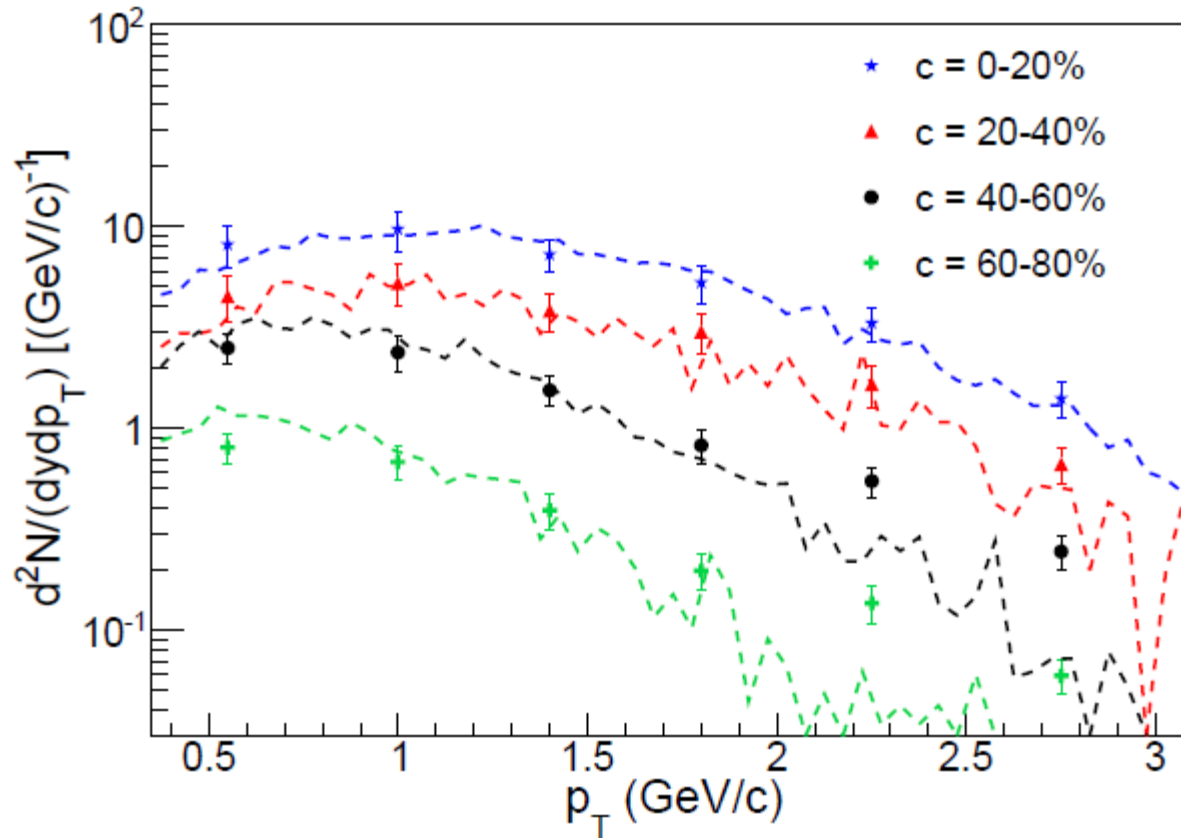


FIG. 3. The fraction of  $K^+\pi^-$  pairs coming from  $K(892)^*$  decay, which can be identified as daughters of  $K^*$  in iHKM simulations after the particle rescattering stage modeled within UrQMD hadron cascade. The simulations correspond to LHC Pb+Pb collisions at  $\sqrt{s_{NN}} = 2.76$  TeV with different centralities. The iHKM results are presented for two cases: the Laine-Shroeder equation of state with particlization temperature  $T_p = 163$  MeV (red line) and the HotQCD equation of state with  $T_p = 156$  MeV (blue line).

## Spectra of $K^{*0}$ (LHC)



The  $K(892)^*$  resonance  $p_T$  spectra for Pb+Pb collision events with different centralities at the LHC energy  $\sqrt{s_{NN}} = 2.76$  TeV obtained in iHKM simulations (lines) in comparison with the experimental data [6] (markers).

## Thermal and evolutionary approaches

# Thermal models vs evolutionary approach

Basic matter properties:  
thermodynamic **EoS**

**Thermal models**

Chemical freeze-out at

$$T_{ch} \approx T_h$$

Particle number ratios

$$\left\{ \frac{N_i}{N_j} \right\}$$

L.-S.  $\rightarrow$  Karsch, Fodor (lattice QCD)

$$T_h = 165 \text{ MeV} \Rightarrow 156 \text{ MeV}$$

**Evolutionary models**

$$\frac{dN_{charge}}{d\eta}(c)$$

$$\frac{dN_\pi}{p_T dp_T}$$

High dense matter formation time  $\tau_0$

Max. energy density  $\epsilon(\tau_0) \equiv \epsilon_0$

At the particlization temperature  $T_{part} \approx T_h$  hydrodynamic evolution transforms (suddenly or continuously) into interact. hadron gas evolution.

**EoS:**

$$\tau_0 = 0.1 \text{ fm/c} \rightarrow 0.15 \text{ fm/c}$$

$$\epsilon_0 = 679 \text{ GeV/fm}^3 \rightarrow 495 \text{ GeV/fm}^3$$

**iHKM**

**Kinetic freeze-out**

«Blast-wave» parametrization of sharp freeze-out hypersurface and transverse flows on it. Spectra  $\frac{dN_i}{p_T dp_T} \rightarrow T_{th}$

«Effective temperature» of maximal emission:  $T_{th}(p)$   
Anyway the kinetic freeze-out in evolutionary models is continuous, how can we check it?

# Continuous freeze-out vs sudden freeze-out

- Thermal models of particle production vs dynamic/evolutionary approaches

## Kinetic/thermal freeze-out

### Sudden freeze-out

Cooper-Frye prescription

$$p^0 \frac{d^3 N_i}{d^3 p} = \int_{\sigma_{th}} d\sigma_\mu p^\mu f_i(x, p)$$

The  $\sigma_{th}$  is typically isotherm.

### Continuous freeze-out

$$p^0 \frac{d^3 N_i}{d^3 p} = \int d^4 x S_i(x, p) \approx \int_{\sigma(p)} d\sigma_\mu p^\mu f_i(x, p)$$

The  $\sigma(p)$  is piece of hypersurface where the particles with momentum near  $p$  has a maximal emission rate.  
*Yu.S. Phys. Rev. C78,*

## Chemical freeze-out

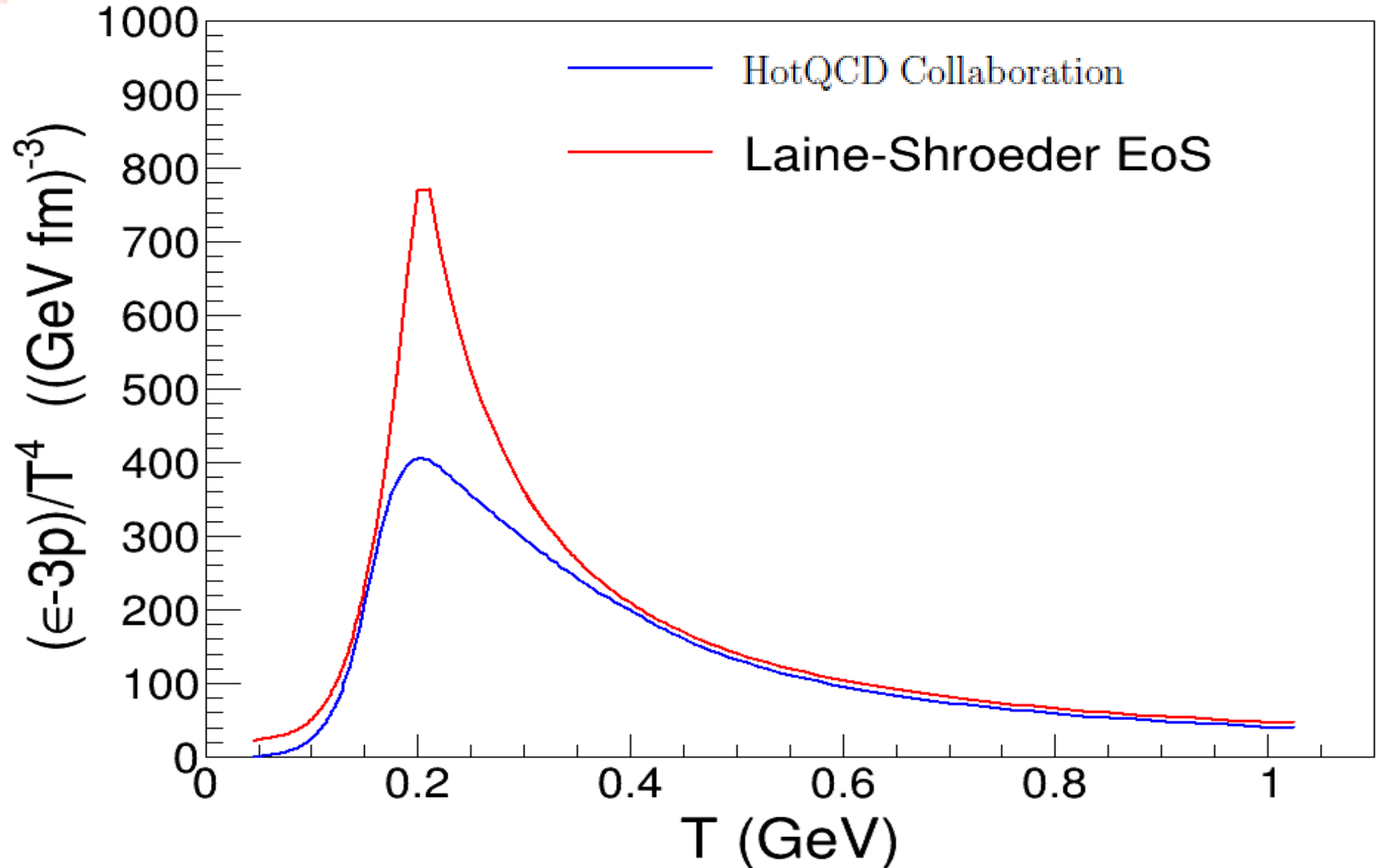
$$N_i = \int_p \int_{\sigma_{ch}} \frac{d^3 p}{p^0} d\sigma_\mu p^\mu f_i\left(\frac{p^\mu u_\mu(x)}{T_{ch}}, \frac{\mu_{i, ch}}{T_{ch}}\right)$$
$$= n_i(T, \mu) V_{eff} \quad V_{eff} = \int_{\sigma_{ch}} u^\mu d\sigma_\mu$$

The numbers of quasi-stable particles is defined from  $N_i$  with taking into account the resonance decays but **not** inelastic re-scattering.

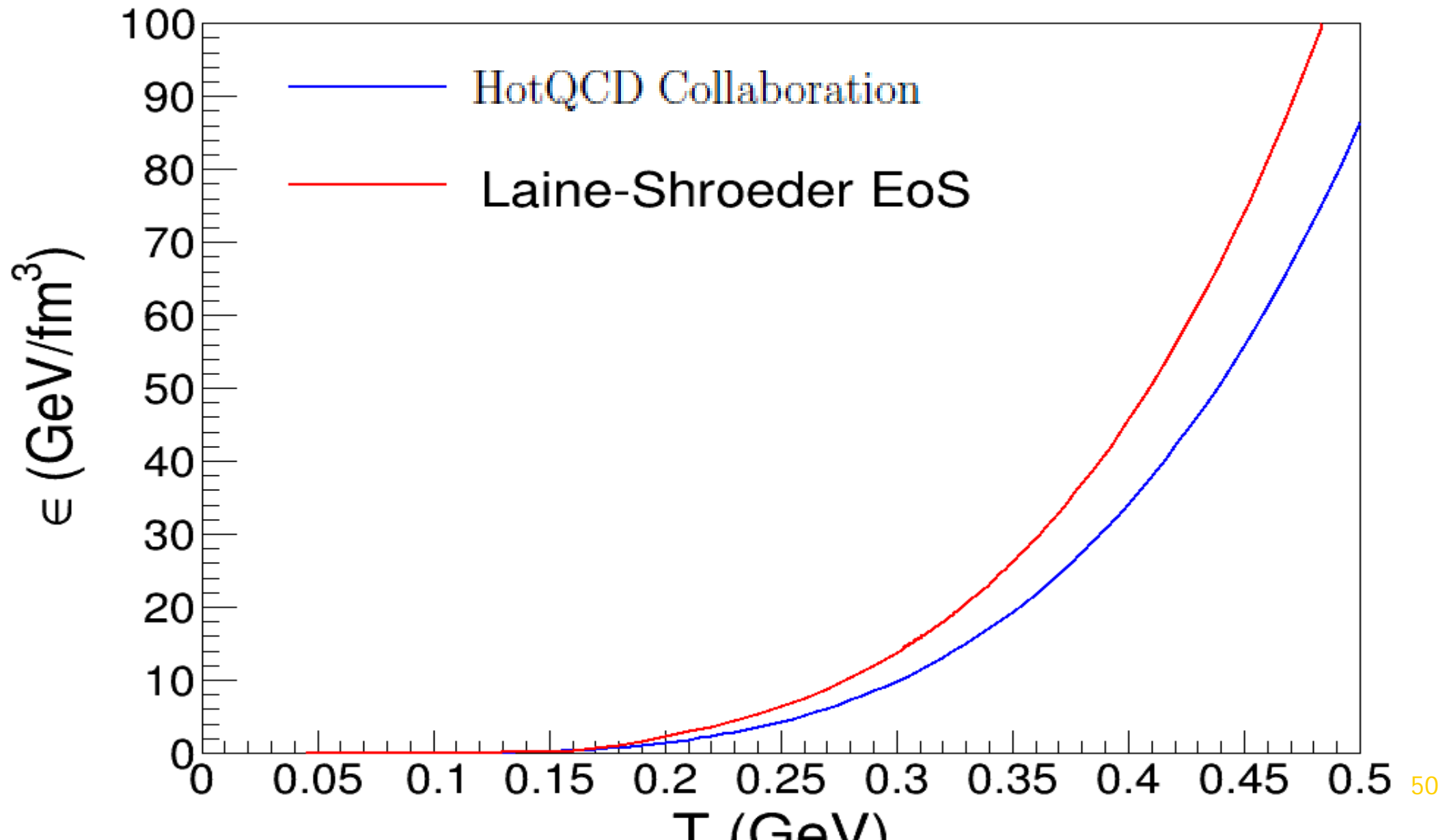
The  $T_{ch}$  is the minimal temperature when the expanding system is still (near) in local thermal and chemical equilibrium. Below the hadronic cascade takes place:  $T_{ch} \rightarrow T_{part}$ . The inelastic reactions, annihilation processes in hadron-resonance gas change the quasi-particle yields in comparison with sudden chem. freeze-out.



# Equation of State - 1

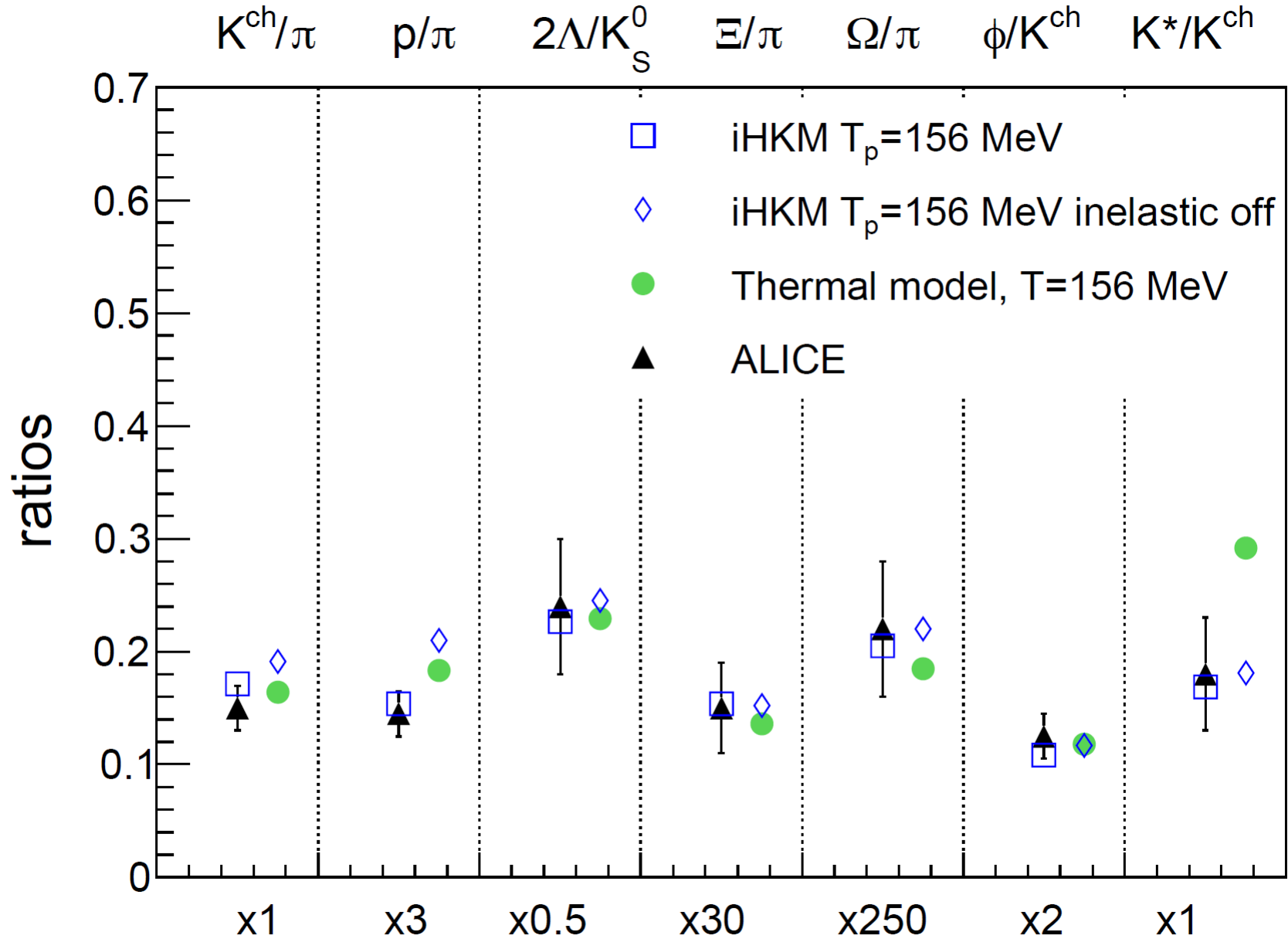


# Equation of state -2

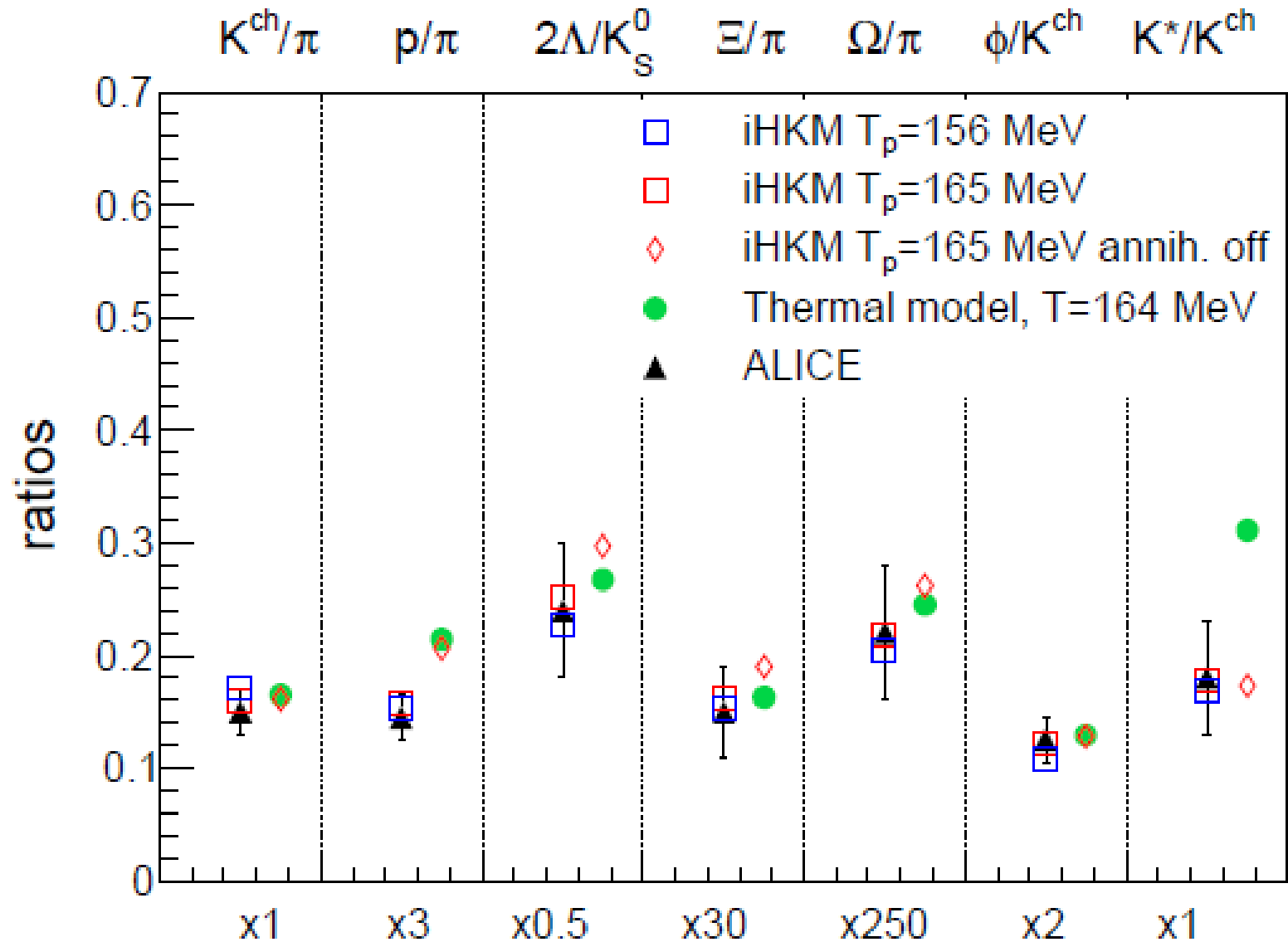


# Particle number ratios at the LHC, Lattice EoS

Yu.S. , Shapoval, arXiv:1708.02389



# Particle number ratios at the LHC, L-S EoS



# Summary on the particle production

- Neither thermal nor chemical freeze-out cannot be considered as sudden at some corresponding temperatures.
- Particle yield probe  $\frac{dN_i}{d\eta} / \frac{dN_j}{d\eta}$  as well as absolute values  $\frac{dN_i}{d\eta}$  (!) demonstrate that even at the minimal hadronization temperature  $T_{ch} = T_h = 156$  MeV, the annihilation and other non-elastic scattering reactions play role in formation particle number ratios, especially.
- It happens that the results for small and relatively large  $T_h$  are quite similar. It seems that inelastic processes (other than the resonance decays), that happen at the matter evolution below  $T_h$  play a role of the compensatory mechanism in formation of  $\frac{dN_i}{d\eta} / \frac{dN_j}{d\eta}$ .  
Chemical freeze-out is continuous.
- As for the thermal freeze-out, the  $K^{*0}(892)$  probes demonstrate that even at the first 4-5 fm/c (proper time!) after hadronization **at least** 70% of decay products are re-scattered. The intensive re-generation of  $K^*$  takes place. **At least** 50% of direct  $K^{*0}(892)$  are re-combine.
- About 30% of much longer-lona-lived resonances  $\phi(1020)$  with hidden strange quark content created additionally to direct  $\phi(1020)$  (coming from hadronization) at the afterburner stage.



# Conclusion

---

To study the matter properties using the strange meson probes at the FAIR and NICA accelerators one needs:

## EXPERIMENT

To provide the measurements of

total multiplicity vs centrality,  
pion and kaon spectra,  
comparative analysis of the femtoscopy radii behavior for pions and kaons,  
particle number ratios in central events,  
 $K^*/K$  and  $\phi/K$  ratios vs centrality

## THEORY

To develop full evolutionary model:

initial state  $\rightarrow$  pre-thermal stage  $\rightarrow$  3D thermal or quasi-thermal expansion of continuous medium (EoS - ?)  $\rightarrow$  particlization  $\rightarrow$  expansion of interacting hadron-resonance gas.

**One of the candidates is iHKM, transformed for reach baryon matter**

Thank you for your attention !

Thanks to Organizers of the Workshop  
for the comprehensive support